



저작자표시-비영리-변경금지 2.0 대한민국

이용자는 아래의 조건을 따르는 경우에 한하여 자유롭게

- 이 저작물을 복제, 배포, 전송, 전시, 공연 및 방송할 수 있습니다.

다음과 같은 조건을 따라야 합니다:



저작자표시. 귀하는 원저작자를 표시하여야 합니다.



비영리. 귀하는 이 저작물을 영리 목적으로 이용할 수 없습니다.



변경금지. 귀하는 이 저작물을 개작, 변형 또는 가공할 수 없습니다.

- 귀하는, 이 저작물의 재이용이나 배포의 경우, 이 저작물에 적용된 이용허락조건을 명확하게 나타내어야 합니다.
- 저작권자로부터 별도의 허가를 받으면 이러한 조건들은 적용되지 않습니다.

저작권법에 따른 이용자의 권리는 위의 내용에 의하여 영향을 받지 않습니다.

이것은 [이용허락규약\(Legal Code\)](#)을 이해하기 쉽게 요약한 것입니다.

[Disclaimer](#)

A Thesis for the Degree of Master of Science

**Characterization of virulence and avirulence activity
of *Ralstonia solanacearum* effector RipB in *Nicotiana
benthamiana***

*Nicotiana benthamiana*에서의 *Ralstonia solanacearum*
이펙터 RipB의 병원성 및 비병원성 특성 연구

FEBRUARY, 2021

LAURA CRISTINA LLANES MELGOZA

MAJOR IN HORTICULTURAL SCIENCE

AND BIOTECHNOLOGY

DEPARTMENT OF AGRICULTURE, FORESTRY

AND BIORESOURCES

THE GRADUATE SCHOOL OF

SEOUL NATIONAL UNIVERSITY

**CHARACTERIZATION OF VIRULENCE AND
AVIRULENCE ACTIVITY OF *Ralstonia solanacearum*
EFFECTOR RIPB IN *Nicotiana benthamiana***

**UNDER THE DIRECTION OF DR. CECILE SEGONZAC
SUBMITTED TO THE FACULTY OF THE GRADUATE SCHOOL
SEOUL NATIONAL UNIVERSITY**

BY

LAURA CRISTINA LLANES MELGOZA

**MAJOR IN HORTICULTURAL SCIENCE AND BIOTECHNOLOGY
DEPARTMENT OF AGRICULTURE FORESTRY AND
BIORESOURCES**

THE GRADUATE SCHOOL OF SEOUL NATIONAL UNIVERSITY

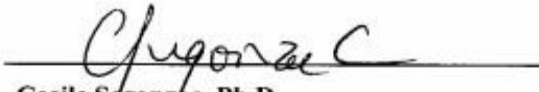
FEBRUARY, 2021

**APPROVED AS A QUALIFIED THESIS OF LAURA CRISTINA LLANES
MELGOZA
FOR THE DEGREE OF MASTER OF SCIENCE
BY THE COMMITTEE MEMBERS**


CHAIRMAN


Kang Byoung Cheorl, Ph.D.

VICE-CHAIRMAN


Cecile Segonzac, Ph.D.

MEMBER


Huh Jin Hoe, Ph.D.

**Characterization of virulence and avirulence activity
of *Ralstonia solanacearum* effector RipB in *Nicotiana
benthamiana*.**

LAURA CRISTINA LLANES MELGOZA

**DEPARTMENT OF AGRICULTURE, FORESTRY AND
BIORESOURCES**

THE GRADUATE SCHOOL OF SEOUL NATIONAL UNIVERSITY

ABSTRACT

Plants rely on innate immunity to perceive and ward off potential pathogens. The perception of pathogen-associated molecular patterns (PAMPs) by pattern recognition receptors leads to PAMP-triggered immunity (PTI) and involves a rapid and strong production of reactive oxygen species (ROS) and massive gene expression change. To circumvent PTI, bacteria produce different classes of virulence factors, in particular type-III secreted effectors (T3E) which are injected into the host cell, thereby providing effector-triggered susceptibility. However, plants possess resistance proteins (R) that recognize the T3Es and initiate the effector-triggered immunity. This triggers a strong defense response which can lead to localized cell

death termed hypersensitive response. *Ralstonia solanacearum* (*Rso*), the causal agent of bacterial wilt in *solanaceous* crops, is one of the most destructive plant bacterial pathogens. *Rso* injects an array of effector proteins called Rips (*Ralstonia*-injected proteins) via its type III secretion system to promote infection. However, the function of these effectors in plant cells remains mostly unknown.

In this study, I selected 36 Rips from 50 previously cloned that are not causing cell death when expressed in *Nicotiana benthamiana* to test their effect on PTI signaling. Transient expression of the selected Rips in *N. benthamiana* shows that several Rips could disturb ROS production triggered by the bacterial PAMP flg22. Interestingly among the four *RipB* alleles present in this screen, three could almost completely suppress flg22-triggered ROS, whereas one could not. Sequence comparison and design of chimeric constructs revealed that the differential effect of *RipB* on flg22-triggered ROS production might be due to the C-terminal domain, present in the three *RipB* alleles suppressing flg22-triggered ROS. *RipB* shares close homology with the *Xantomonas* and *Pseudomonas* effector protein XopQ and

HopQ1, respectively, which are recognized by the plant resistance protein Roq1. In Roq1 silenced plants, the *RipB* allele with the C-terminal region could not be recognized although it could still suppress flg22-triggered ROS production. Together these results give a glimpse of how *RipB* alleles are modulating the immune responses in *N. benthamiana*, however, more studies are needed to understand the pathway it follows.

Key Words: reactive oxygen species, *Ralstonia solanacearum*, *Nicotiana benthamiana*, effectors, PTI, ETI, RipB, Plant immunity

Student number: 2019-23541

CONTENTS

ABSTRACT	i
CONTENTS	iv
LIST OF TABLES	vi
LIST OF FIGURES	vii
LIST OF ABBREVIATIONS	ix
INTRODUCTION	1
MATERIAL AND METHODS	6
Plant materials	6
<i>Agrobacterium tumeraciences</i> -mediated transient expression assays (agroinfiltration)	6
Measurement of ROS production	7
Semiquantitative RT-PCR/ quantitative PCR	8
Western blotting	9
Virus-induced Gene Silencing (VIGS)	10
Cell death quantification	10

RESULTS	13
Screening for <i>Ralstonia solanacearum</i> effectors that modulate plant PTI responses	13
<i>RipB</i> alleles modulate flg22 but not chitin-triggered ROS burst	18
<i>RipB</i> alleles are differentially recognized in <i>N.</i> <i>benthamiana</i>	19
Determination of the RipB domain required for flg22- induced ROS burst suppression and/or recognition in <i>N.</i> <i>benthamiana</i>	26
Roq1 silencing in <i>N.benthamiana</i> to assess in Roq1 recognition of RipB effectors is the reason for ROS burst suppression	33
DISCUSSION	40
REFERENCES	46
ABSTRACT IN KOREAN	65

LIST OF TABLES

Table 1. List of primers

Table 2. *Ralstonia solanacearum* effector collection and characteristics

LIST OF FIGURES

Figure 1. Several *Rso* effectors modulate flg22-triggered ROS production in *N. benthamiana*

Figure 2. *RipB* alleles differentially modulate flg22 and chitin-triggered ROS production in *N. benthamiana*

Figure 3. Expression of the different *RipB* alleles (*Rs8*, *Rs9*, *Rs10* and *Rs27*) in *N. benthamiana*.

Figure 4. Several *RipB* alleles are recognized in *Nicotiana spp.*

Figure 5. Natural variation in the *RipB* alleles sequences

Figure 6. Schematic representation of *RipB* protein domains and *RipB* chimeric proteins

Figure 7. Expression of *RipB* chimeric constructs in *N. benthamiana*.

Figure 8. *RipB* C-terminal region is necessary for flg22-ROS burst suppression in *N. benthamiana*.

Figure 9. RipB' s C-terminal is required for the induction of cell death in *Nicotiana spp.*

Figure 10. Characterization of *Roq1*-silenced plants

Figure 11. *Roq1* might be involved in RipB' s C-terminal recognition leading to cell death

Figure 12. RipB suppression of ROS burst might not be linked with RipB recognition by *Roq1*

LIST OF ABBREVIATIONS

<i>A. tumefaciens</i>	<i>Agrobacterium tumefaciens</i>
Avr	avirulence
ETI	effector-triggered immunity
ETS	effector-triggered susceptibility
GFP	Green fluorescent protein
HR	hypersensitive response
MAPK	mitogen-activated protein kinase
<i>N. benthamiana</i>	<i>Nicotiana benthamiana</i>
<i>N. tabacum</i>	<i>Nicotiana tabacum</i>
NLR	nucleotide-binding leucine-rich repeat
OD	optical density
PAMP	pathogen-associated molecular pattern
PRR	pattern recognition receptor
PTI	PAMP-triggered immunity
R gene	resistance gene
Rips	Ralstonia-injected proteins
RLU	relative light unit
R protein	resistance protein

<i>Rso</i>	<i>Ralstonia solanacearum</i>
<i>R. solanacearum</i>	<i>Ralstonia solanacearum</i>
semi qRT-PCR	Semi-quantitative RT-PCR
T3E	type-III secreted effectors
T3SS	type III secretion system
TRV	tobacco rattle virus
VIGS	virus-induced gene silencing

INTRODUCTION

Ralstonia solanacearum (*Rso*) is a Gram-negative, soil-borne bacteria that causes bacterial wilt disease in crops such as potato, tomato and pepper (Zhao et al., 2019). This bacterium is one of the most destructive pathogens due to its wide geographical distribution, large heterogeneity and aggressiveness (Sun et al, 2019). The rapid proliferation of bacteria in the xylem blocks the water transportation of the host plant, which results in the wilting and death of infected plants (Lowe-Power et al., 2018). Many Gram-negative bacteria, including *Rso*, depend on the Hrp type III secretion system for pathogenicity; this system injects bacterial virulence proteins (effector also termed *Ralstonia* injected proteins - Rips) into plant cells (Galán et al., 2014). Type III effectors manipulate host cellular processes to suppress plant immunity, to secure nutrients and to provide a favorable environment for pathogen growth (Büttner, 2016).

Plants have a developed immune system to respond to infection, employing external and internal receptors (Jones and Dangl 2006). Plants rely on surface-localized pattern recognition receptors

(PRRs) to detect conserved molecules called pathogen/microbe-associated molecular patterns (PAMPs) (Boller and Felix 2009). Based on the recognition mechanism of invading pathogens, the plant immune system can be divided into pattern-triggered immunity (PTI), which is considered to be the first level of plant defense, and effector-triggered immunity (ETI) (Jones and Dangl 2006). In PTI, plants detect potential pathogens by recognizing PAMPs, such as flagellin or chitin, through the PRRs on the cell surface (Macho and Zipfel 2014). PAMPs recognition induce defense responses including generation of reactive oxygen species (ROS), a burst of Ca^{2+} , post-translational activation of mitogen-activated protein kinases (MAPKs), expression of defense-related genes, callose deposition into plant cell walls, and production of antimicrobial compounds and cell-wall-reinforcing materials around the infection site (Halhlbrock *et al.*, 2003), ultimately limiting pathogen colonization and infection (Couto and Zipfel 2016; Kunze *et al.*, 2004; Chinchilla *et al.*, 2006). Evidence shows that ROS are generated in various sub-cellular compartments shortly after pathogen recognition. ROS have been found to have a central role in

plant immune signaling, besides regulating diverse cellular processes. One of these processes is programmed cell death, considered to be the result of ROS triggering a physiological or programmed pathway (Mittler, 2017; Qi, Wang, Gong, & Zhou, 2017; Zurbriggen, Carrillo, & Hajirezaei, 2010).

Type III effectors (T3Es) contribute collectively to bacterial pathogenesis by targeting host defense pathways and hijacking multiple cellular processes (Katagiri et al., 2002). Suppression of PTI is a primary role of bacterial effectors to ensure pathogenesis. For example, AvrPto and AvrPtoB from *Pseudomonas syringae* directly suppress PRR activation (Gimenez-Ibanez et al., 2018), RipAY from *Rso* targets redox regulators (Mukaihara et al., 2016; Sang et al., 2018; Fujiwara et al., 2016), and HopQ1, which contains a nucleoside hydrolase (NH) domain, contributes to PTI suppression by reducing expression of the PRR *FLS2* (Hann et al., 2014).

Plants have evolved resistance (R) proteins that recognize effector intracellularly and induce effector-triggered immunity (ETI) (Dodds and Rathjen 2010; Chisholm et al., 2006). The nucleotide-

binding domain and leucine-rich repeats (NLR) family of intracellular receptors detect the presence of effectors, triggering potent immune responses (Jacob *et al.*, 2013). ETI defense responses are similar yet prolonged and stronger than PTI responses, and often accompanied by hypersensitive response (HR), which is a rapid and localized cell death at the site of infection. One model for the activation of an NLR protein by an effector is through physical interaction between the effector protein and the cognate NLR receptor, which involves the formation of a protein complex. For instance, Roq1 can physically associate with HopQ1 and its close homolog XopQ that shares the NH domain (Schultink *et al.*, 2017). Alternatively, NLR recognition can be based on the activity of an effector, in which NLR protein is activated when it detects perturbations (Schultink, *et al.*, 2017). The pathogen effectors recognized by plant R proteins are called avirulence (Avr) proteins, as their recognition restrict virulence of the pathogen to specific hosts hence determining the host-range specificity of a pathogen (Cui *et al.*, 2015).

In this study four alleles of the *Rso* effector RipB obtained from Korean strains (*Rs8*, *Rs9*, *Rs10* and *Rs27*) were analyzed by transient expression in leaves of *N. benthamiana* in order to identify RipB virulence and avirulence activities. I focused on the modulation of physiological responses such as ROS burst, HR and expression of defense-related marker genes. Additionally, among the four alleles, *Rs8* presents a shorter sequence, lacking the C-terminal region present in *Rs9*, *Rs10*, *Rs27*, and in the close homologs HopQ1 and XopQ, hence likely lacking the functional NH domain predicted from sequence comparison. For this reason, the role of RipB C-terminal region in the modulation of plant immune responses was also evaluated. During the course of my research, a publication characterizing RipB from a Japanese *Rso* strain (Nakano & Mukaihara, 2019) demonstrated that the *N. benthamiana* NLR protein Roq1 is involved in RipB recognition. Therefore, the recognition of the Korean *RipB* alleles by *Roq1* was also evaluated.

MATERIALS AND METHODS

Plant materials

N. benthamiana plants were grown for 5 to 6 weeks in a growth chamber at 24 to 26°C with a relative humidity of 60%, under 16 h light/ 8 h dark cycle.

Agrobacterium tumefaciens- mediated transient expression assays (agroinfiltration)

For transient effector expression in *N. benthamiana*, *A. tumefaciens* AGL1 cells containing the respective effector and control constructs were grown at 28°C for 48 h in LB broth low salt media (Duchefa Biochemie, Haarlem, The Netherlands) solidified with agar (Georgiachem, Gangwon-do, Korea) containing carbenicillin and spectinomycin (for GFP construct) or carbenicillin and kanamycin (for effectors constructs) as selective antibiotics. A single colony was used to inoculate 3 ml of liquid LB broth low salt media with the corresponding selective antibiotics and grown overnight at 28°C. Next, 2 ml of liquid culture were centrifuged at 8000 rpm for 3 min and the

supernatant was discarded. Collected cells were resuspended in infiltration medium (10 mM MgCl₂ and 10 mM MES-KOH, pH=5.6) to reach an optical density (OD) of 0.5 at 600 nm. This suspension was infiltrated in fully expanded leaves of 5-6 week- old plants.

Measurement of ROS production

Leaf discs of agroinfiltrated *N. benthamiana* were collected using 5 mm diameter biopsy punch. The leaf discs were floated on 150 µl of demineralized water overnight, then the water was replaced with 100 µl of assay solution containing 100 µM luminol (Sigma-Aldrich, Missouri, USA) and 2 µg of horseradish peroxidase (Sigma-Aldrich). ROS was elicited with 50 nM flg22 (Pepton, Daejeon, Korea), or 100 µg/ml of chitin (Sigma). ROS burst production was measured using a chemiluminescence plate reader (GloMax 96 Microplate Luminometer, Promega). Luminol oxidation was expressed in relative light unit (RLU) over a period of 75 minutes.

Semiquantitative/quantitative RT-PCR

Agroinfiltrated *N. benthamiana* leaf discs were collected at 1 day post-inoculation (dpi) and frozen in liquid nitrogen, or floated on water overnight and then treated with water, 50 nM flg22 or 100 µg/ml of chitin for 30 minutes and frozen in liquid nitrogen. Total RNA was extracted using TRIzol-Reagent (Ambion, Texas, USA) and treated with DNase I (Sigma-Aldrich). First-strand cDNA was synthesized from 2.5 µg of RNA using Maxima first strains cDNA synthesis kit (Thermo Scientific, Massachusetts, USA). For quantitative RT-PCR, 4 µl of diluted cDNA were combined with Prime Taq Polymerase kit (Genet Bio, Daejeon, Korea). PCRs were performed for two biological repeats. Samples were run in 2% Agarose gel (Georgiachem) and ImageJ software was used to quantify the intensity of the bands on the gel pictures. Expression of defense marker genes was normalized by that of *NbEF1α*.

For quantitative RT-PCR, 4 µl of cDNA were combined with GoTaq qPCR master mix (Promega). PCR reactions were performed

in triplicate for two biological repeats. Expression of defense marker genes was normalized by that of *NbEF1a*.

Western blotting

Agroinfiltrated *N. benthamiana* leaves were collected 24 h after infiltration and frozen in liquid nitrogen. For protein extraction, a buffer was made with 30 ml of GTEN (10% glycerol, 50 mM TRIS pH=7.5, 2 mM EDTA pH=8 and 150 mM NaCl), $\frac{3}{4}$ tablet of complete protease inhibitor (Sigma), 0.2% of Igepal (Sigma), 1% of Polyvinylpolypyrrolidone (PVPP) and 5 mM of Dithiothreitol (DTT) (Sigma). Previously frozen leaves were grinded and as soon as defreeze on ice, resuspended on 3 ml of extraction buffer to isolate total protein samples. Then protein samples were separated electrophoretically by SDS-PAGE and transferred onto a PVDF membrane. The membrane was blocked with 5% skim milk in TBST (100 ml Tris-Buffered Saline with 5 ml Tween 20% and diluted to 1 L) overnight at 4°C. Then the membrane was washed with TBST for 10 minutes 3 times and once with TBS (Tris-Buffered Saline) for 10

minutes. The membrane was incubated with Anti-FLAG-HRP conjugated antibodies for 1 hour 30 minutes at room temperature (RT). The bound antibodies were detected by the chemiluminescence with Azure 400 Visible Fluorescent Western Blot Imaging system (Azure Biosystems). Then membrane was stained with Ponceau S solution (Sigma).

Virus-induced Gene Silencing (VIGS)

Tobacco rattle virus (TRV)-based VIGS was used, in which pTRV1 encodes the replication and movement viral functions and pTRV2 harbors the coat protein and the sequence used for VIGS. *Agrobacterium tumefaciens* (OD_{600 nm} 0.5) containing pTRV1, pTRV2-EV (Empty Vector) or pTRV2-Roq1 were used to infiltrate 2 weeks old *N. benthamiana* cotyledons. Plants were further kept in the growth chamber for 3 weeks before the experiments.

Cell death quantification

N. benthamiana leaves were agroinfiltrated and at 6 dpi chlorophyll fluorescence kinetics for each spot was measured with Closed FluorCam FC 800-C (Photon Systems Instruments). Two biological repeats with six technical repeats were performed, each one using three *N. benthamiana* plants, two leaves per plant, infiltrating four spots per leaf.

Table 1. List of primers			
Gene		Sequence (5'→3')	Purpose
NbEF1 α	F	AAGGTCCAGTATGCCTGGGTGCTTGAC	semi-qRT-PCR
	R	AAGAATTCACAGGGACAGTTCCAATACCAC	semi-qRT-PCR
NbCYP71D20	F	AAGGTCCACCGCACCATGTCCTTAGAG	quantitative-PCR
	R	AAGAATTCCTTGCCCCTGAGTACTTGC	quantitative-PCR
NbRoq1	F	GAATTCATTCGACAAATTTTGTCTCT	Gene silencing
	R	GGATCCTCTACAAATTCTACCTCAACAGTTTGG	Gene silencing
NbRoq1	F	TGCCACAACGATGTCAGTCA	quantitative-PCR
	R	CTTGAGCTCTTCAGTCCGCA	quantitative-PCR
NbHin1	F	GCTTGGTTTTATTGGGAGAT	quantitative-PCR
	R	ATGATCTGCCATTAGACCCT	quantitative-PCR
NbHsr203J	F	GGAGGAGCTTAAATTGCCGC	quantitative-PCR
	R	TTCAGAACCAGTTACAGGGT	quantitative-PCR
NbACRE31	F	AAGGTCCCGTCTTCGTCGGATCTTCG	quantitative-PCR
	R	AAGAATTCGGCCATCGTGATCTTGGTC	quantitative-PCR
NbACRE132	F	AAGGTCCAGCGAAGTCTCTGAGGGTGA	quantitative-PCR
	R	AAGAATCCAATCCTAGCTCTGGCTCCTG	quantitative-PCR
NbEF1 α	F	TGGACACAGGGACTTCATCA	quantitative-PCR
	R	CAAGGGTGAAAGCAAGCAAT	quantitative-PCR

RESULTS

Screening for *Ralstonia solanacearum* effectors that modulate plant PTI responses

Ralstonia solanacearum (Rso) strains were isolated from tomato (To) or pepper (Pe) diseased fields across South Korea and their genome sequenced (Segonzac et al., 2017; Prokchorchik *et al.*, 2020). From these strains, effector (*Rip*) sequences were used to predict the encoded protein size (using Geneious sequence analysis software) and the conserved domains (using NCBI Conserved Domain Database) (Table 2). Among the domains found are: i) TAL effector, which binds to DNA (Bai *et al.*, 2000 and Nga-Sze Mak *et al.*, 2012); ii) Peptidase M91, which contains an HEXXH motif (Baruch *et al.*, 2011), iii) nucleoside hydrolases (Degano *et al.*, 1996); iv) leucine rich repeat (LRR) ; v) F-box, a receptor for ubiquitination targets (Bai *et al.*, 1996); vi) LRR RI capping, capping unit of ribonuclease inhibitors of leucine rich repeat (Lomax *et al.*, 2014); vii) acetyltransferase 14 (Yoon *et al.*, 2003); viii) Nuc hydro 2, a subgroup of nucleoside hydrolases

(Degano *et al.*, 1996); ix) DUF3348, domain of unknown function; x) GGCT, which is a gamma-glutamyl cyclotransferase (Oakley *et al.*, 2008); xi) HAD like, haloacid dehalogenase-like hydrolases (Hisano *et al.*, 1996); xii) AMN1, antagonist of mitotic exit network protein 1 (Wang *et al.*, 2006); xiii) flhF, flagellar biosynthesis protein FlhF; and xvi) nudix hydrolase, that catalyzes the hydrolysis of nucleoside diphosphates (McLennan 2006). Among the 36 effectors, 22 have predicted domains, while the remaining 14 did not have homologies to known domains. Based on data from Boyoung Kim (Horticultural Crop Molecular Physiology Laboratory, Seoul National University) about cell death induced after transient expression of Rso effectors in *N. benthamiana* (Nb) or *N. tabacum* (Nt) (table 2), the effectors that did not cause cell death in Nb were selected for functional study.

PTI induction leads to a variety of defense responses, including the generation of reactive oxygen species (ROS) (Zurbriggen *et al.*, 2016). To test if Rso effectors listed in Table 2 could modulate ROS production, ROS burst was elicited by flg22

in *N. benthamiana* leaf discs transiently expressing each effector (Figure 1). Total ROS production during 75 min following flg22 treatment was measured, and the experiment was repeated 2 or 3 times in different batches of plants (Figure 1A). GFP that has a broad use in transient expression systems (Chiu *et al.*, 1996) and was used as a positive control, while a type III secreted effector from *Pseudomonas syringae* (AvrPtoB), which blocks all defense responses, (Gimenez-Ibanez *et al.*, 2009) was used as a negative control. Statistically significant (according to Student's t-test) reduction or enhancement of ROS production was observed when certain Rips were expressed. Expression of effectors Rs16, Rs26, Rs31, Rs35 and Rs37 lead to higher flg22-ROS production (Figure 1B). Expression of effectors Rs9, Rs10, Rs20, RS27, Rs34 and Rs38 lead to lower flg22-ROS production (Figure 1C) compared to GFP. Comparing the predicted domains it was observed that Rs16, Rs31 (ROS enhancement) and Rs34 (ROS suppression) have LRR domains (Table 2). On the other hand, Rs9, Rs10 and Rs27 (ROS reduction) share a nucleoside

hydrolase (NH) domain. However only these mentioned effectors had domains in common, Rs37 and Rs38 did not share predicted domains, while Rs26, Rs35 and Rs20 had no predicted domains. Therefore, no predicted function could be associated with ROS modulation by these effectors. Of note, Rs34 (RipAC) expression has been found to almost completely block the early ROS production (Yu *et al.*, 2020), similarly to Rs38 (RipAY), which has been observed to strongly reduce flg22-triggered ROS burst (Sang *et al.*, 2018), confirming the observed results in Figure 1C.

Rs9, Rs10 and Rs27, which were found to suppress ROS burst, share the NH domain, truncated in Rs8, which apparently does not affect ROS production. Considering the obtained results, these alleles of the same effector, RipB, were selected for further analysis in order to determine how RipB modulates defense responses.

Effector #	Representative Strain ^A	Protein size (aa)	Domain prediction ^B	Cell death-inducing ^C
Rs1	Pe_1	1245	TAL	-
Rs3	Pe_1	436	-	-
Rs4	Pe_1	1273	-	-
Rs5	To_7	99	-	-
Rs6	Pe_1	393	Peptidase_M91	-
Rs7	To_7	277	-	-
Rs8	Pe_1	393	nuc_hydro	-
Rs9	To_7	452	nuc_hydro	Nt
Rs10	Pe_57	518	nuc_hydro	Nt
Rs11	Pe_1	140	-	-
Rs13	Pe_1	661	F-box and LRR	-
Rs14	Pe_4	507	LRR_RI	-
Rs15	Pe_1	620	LRR	-
Rs16	To_7	643	LRR_RI	-
Rs17	Pe_1	430	Acetyltransf_14	-
Rs19	To_7	503	-	-
Rs20	Pe_9	1067	-	Nb
Rs21	Pe_9	96	-	-
Rs22	Pe_9	218	Peptidase_M91	-
Rs24	Pe_4	98	-	-
Rs25	Pe_9	273	Peptidase_M91	-
Rs26	Pe_9	255	-	-
Rs27	Pe_9	490	nuc:hydro	Nt
Rs28	Pe_9	184	-	-
Rs30	Pe_9	431	Acetyltransf_14	-
Rs31	Pe_42	621	LRR	-
Rs33	Pe_1	174	-	Nb
Rs34	Pe_1	984	LRR	-
Rs35	Pe_1	203	-	-
Rs37	Pe_1	246	DUF3348 superfamily	-
Rs38	Pe_1	416	GGCT_like superfamily	-
Rs43	Pe_2	943	HAD_like	-
Rs44	Pe_1	1035	LRR_RI, AMN1	-
Rs46	Pe_2	608	LRR_RI	-
Rs48	Pe_1	474	flhF superfamily and Nudix_Hydrolase_29	-
Rs49	Pe_1	292	-	-

Table 2. *Ralstonia solanacearum* effector collection and characteristics.

^A*Rso* strains were isolated from tomato (To) or pepper (Pe) diseased fields across Korea (Segonzac et al., 2017; Prokhorchik et al., 2020).

^BDomain prediction result from conserved domain search on NCBI Conserved Domain Database (<https://www.ncbi.nlm.nih.gov/Structure/cdd/wrpsb.cgi>). Abbreviations: TAL: Transcription activator-like; nuc hydro: nucleoside hydrolases, LRR: Leucine-rich repeats; LRR_RI: Leucine-rich repeats ribonuclease inhibitors capping unit; DUF: domain of unknown function; GGCT: Gamma-glutamyl cyclotransferase; HAD: Haloacid dehalogenase-like hydrolases; flhF superfamily: flagellar biosynthesis protein; F-box: receptor for ubiquitination targets; (-): no domain predicted.

^CCell death induced after transient expression of effectors in *N. benthamiana* (Nb) or *tabacum* (Nt) (data from Boyoung Kim, Horticultural Crop Molecular Physiology Laboratory, SNU).

***RipB* alleles modulate flg22- but not chitin-triggered ROS burst.**

Using the 4 *RipB* alleles (Rs8, Rs9, Rs10 and Rs27) present in the screening, flg22- triggered ROS burst was measured again (Figure 2A), in *N. benthamiana* leaf discs transiently expressing them, obtaining similar results. ROS production was observed to be reduced in the presence of Rs9, Rs10 and Rs27, and no significant modulation was observed with Rs8.

Chitin is a component of fungal cell wall that act as PAMPs on plant cells (Gimenez-Ibanez *et al.*, 2009). To determine if *RipB* expression affects chitin- triggered ROS burst, it was measured in *N. benthamiana* leaf discs transiently expressing each *RipB* allele (Figure 2B). In three biological repeats, no significant effect was observed, indicating that *RipB* alleles affect flg22- but not chitin-triggered ROS burst. On the other hand, in leaf discs from mock treatment there was no significant difference between *RipB* alleles compared to GFP control, therefore *RipB*

expression does not lead to accumulation of constitutive ROS (Figure 2C).

Expression of RipB proteins was confirmed by western blotting (Figure 3), which demonstrates that the absence of effect of Rs8 on ROS production is not due to the differences in protein expression, but rather is the result of differences among the allele sequences.

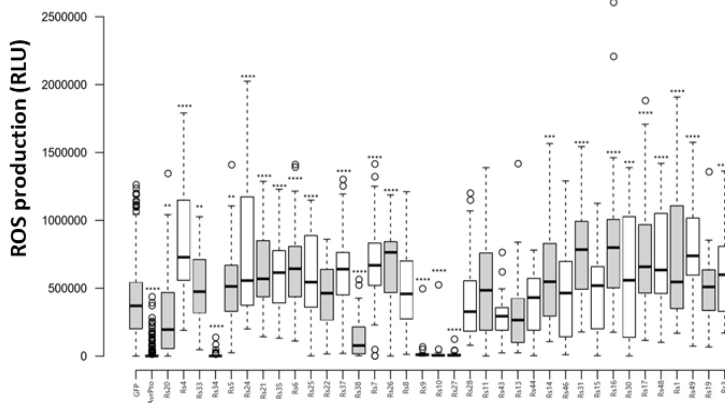
***RipB* alleles are differentially recognized in *N. benthamiana*.**

Localized cell death, called hypersensitive response (HR), is one of the cellular events known to be associated with PTI and ETI (Dodds *et al.*, 2010). RipB (obtained from a Japanese strain of *Ralstonia solanacearum*) has been described as a major avirulence effector in *N. benthamiana* (Nakano *et al.*, 2019) which is probably recognized by the NLR protein Roq1. In this study RipB expression did not induce cell death but induced constitutive ROS accumulation and defense-associated gene expression (Nakano *et al.*, 2019).

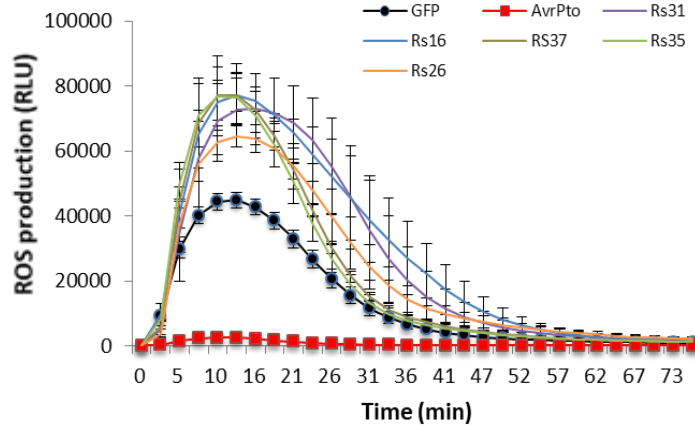
Additionally, in previous experiments done by Boyoung Kim (Horticultural Crop Molecular Physiology Laboratory, Seoul National University) RipB expression induced cell death in *N. tabacum* but not in *N. benthamiana*. During my experiment, no cell death was observed at 2 dpi prior to ROS burst measurement. To test if the *RipB* alleles (obtained from Korean strains of *Ralstonia solanacearum*) are recognized in *N. benthamiana*, cell death and gene expression changes were monitored. To evaluate if the expression of *RipB* alleles induced HR, *N. benthamiana* and *N. tabacum* leaves were transiently infiltrated and chlorophyll fluorescence kinetics for each area was measured at 6 dpi (Figure 4 A-F), a longer period of time than the one for ROS burst experiment. It has been reported that RipE1 triggers cell death (Sang *et al.*, 2020 and Jeon, Kim *et al.*, 2020) therefore RipE1 was used as a positive control. Results showed cell death at 6 dpi in areas infiltrated with Rs9 (6/6 spots), Rs10 (4/6 spots) and Rs27 (3/6 spots) while Rs8 did not induce significant cell death compared with GFP (Figure 4 A, B, D and E). However, cell

death was not constantly observed, probably due to protein accumulation. Furthermore, expression of Rs9, Rs10 and Rs27 induced the expression of ETI-marker genes *NbHin1* (Pontier *et al.*, 1994) and *NbHsr203J* (Gopalan *et al.*, 1996) (Figure 4 G-H). Together these results suggest that Rs9, Rs10 and Rs27 are probably recognized by a R gene in *N. benthamiana* and their expression leads to induction of ETI-marker genes. Furthermore, there must be differences among *RipB* allele sequences that lead to the different effects observed.

A



B



C

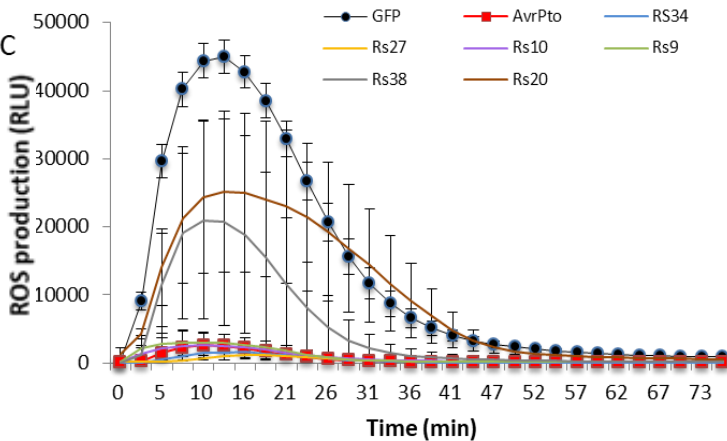


Figure 1. Several *Rso* effectors modulate flg22-triggered ROS production in *N. benthamiana*.

(A) ROS burst elicited by flg22 was measured in *N. benthamiana* leaf disc transiently expressing the different effectors. Boxplots represent the distribution of the total ROS production measured during 75 minutes in two or three biological repeats for each effector (n=32 or n=48). GFP (n=352) and *P. syringae* effector AvrPto (n=352) were used as controls. (B) and (C) Kinetic of ROS production measured in *N. benthamiana* expressing effectors leading to higher (B) or lower (C) flg22-ROS production compared to GFP. Data are means of three biological repeats with error bars representing the standard error of the mean SEM (n=32 or n=48 for effectors and n=352 for GFP and AvrPto). Statistical significance compared to leaf expressing GFP is indicated by asterisks (Student's t-test, $p < 0.0001$ ****, $0.0001 < p < 0.001$ ***, $0.001 < p < 0.01$ **, $0.01 < p < 0.05$ *).

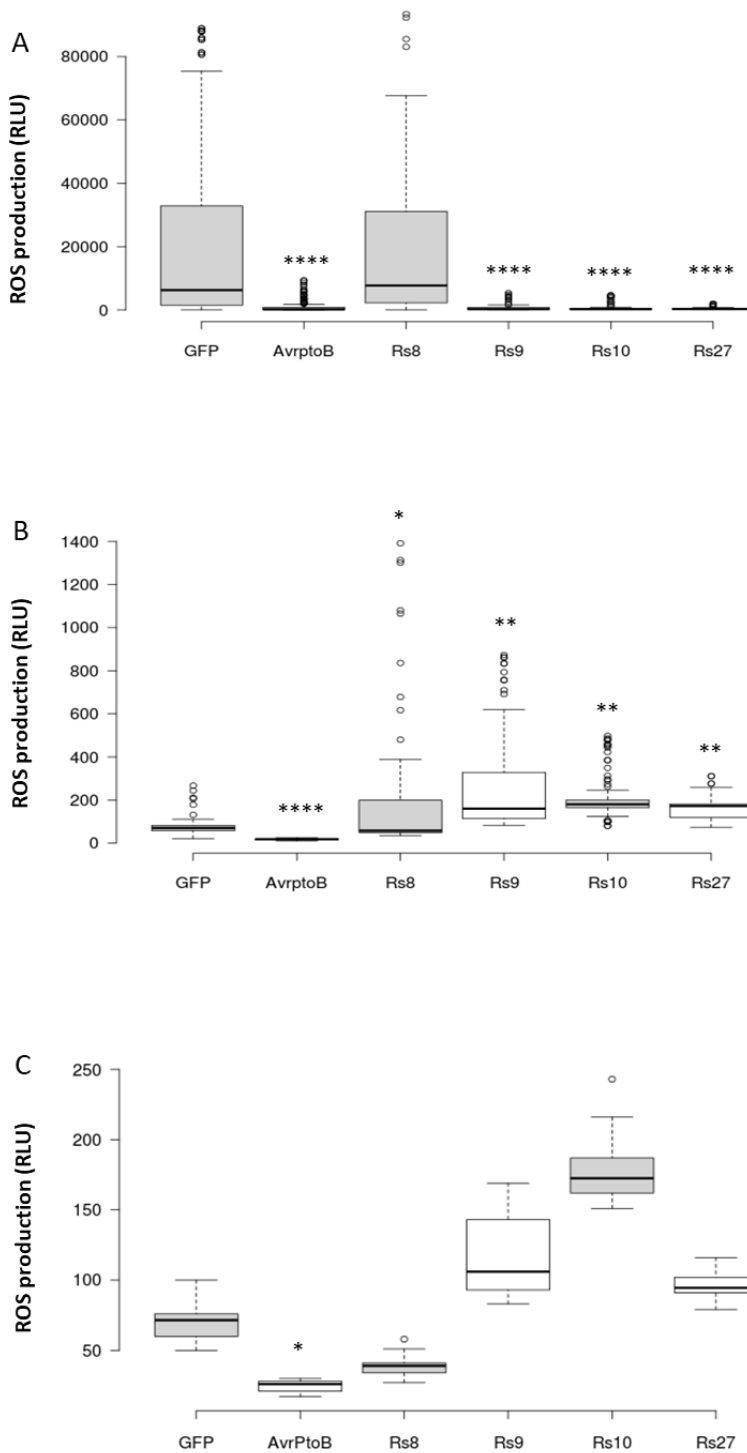


Figure 2. *RipB* alleles differentially modulate flg22 and chitin- triggered ROS production in *N. benthamiana*.

ROS burst was elicited by 50 nM flg22 (A), 100 ug/ml chitin (B) or water (C) in *N. benthamiana* transiently expressing the four *RipB* alleles (Rs8, Rs9, Rs10 and Rs27). GFP and AvrPtoB were used as positive and negative controls respectively. Data are means of three biological repeats with error bars representing the SEM (n=64 or n=80 for effectors and n=144 for GFP and AvrPtoB). Statistical significance compared to leaf expressing GFP is indicated by asterisks (Student's t-test, p<0.0001 ****, p=0.0001<p<0.001 ***, 0.001<p<0.01**, 0.01<p<0.05*).

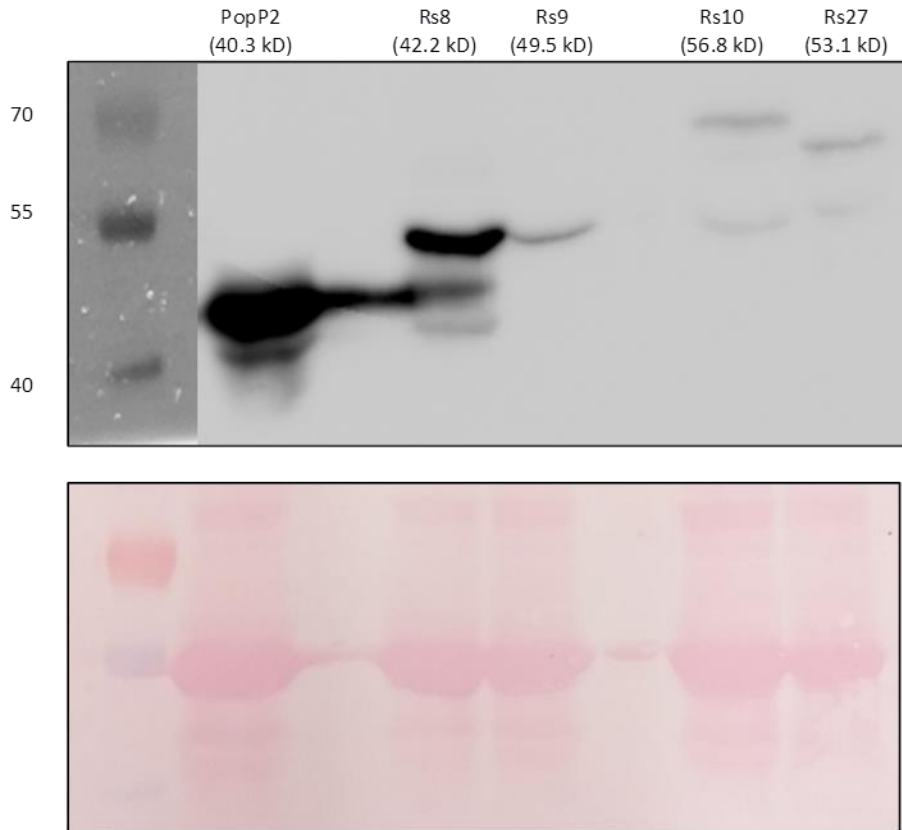


Figure 3. Expression of different *RipB* alleles (*Rs8*, *Rs9*, *Rs10* and *Rs27*) in *N. benthamiana*. *Rs8*, *Rs9*, *Rs10* and *Rs27* were agroinfiltrated in *N. benthamiana* and harvested 2 days post-infiltration. Western blot with anti-flag antibody show *Rs8*, *Rs9*, *Rs10* and *Rs27* proteins (top panel). After revealing, membrane was stained Ponceau S (bottom panel). Ladder used is shown on the left. Predicted molecular weights are below the samples names. PopP2-FLAG protein was included as control.

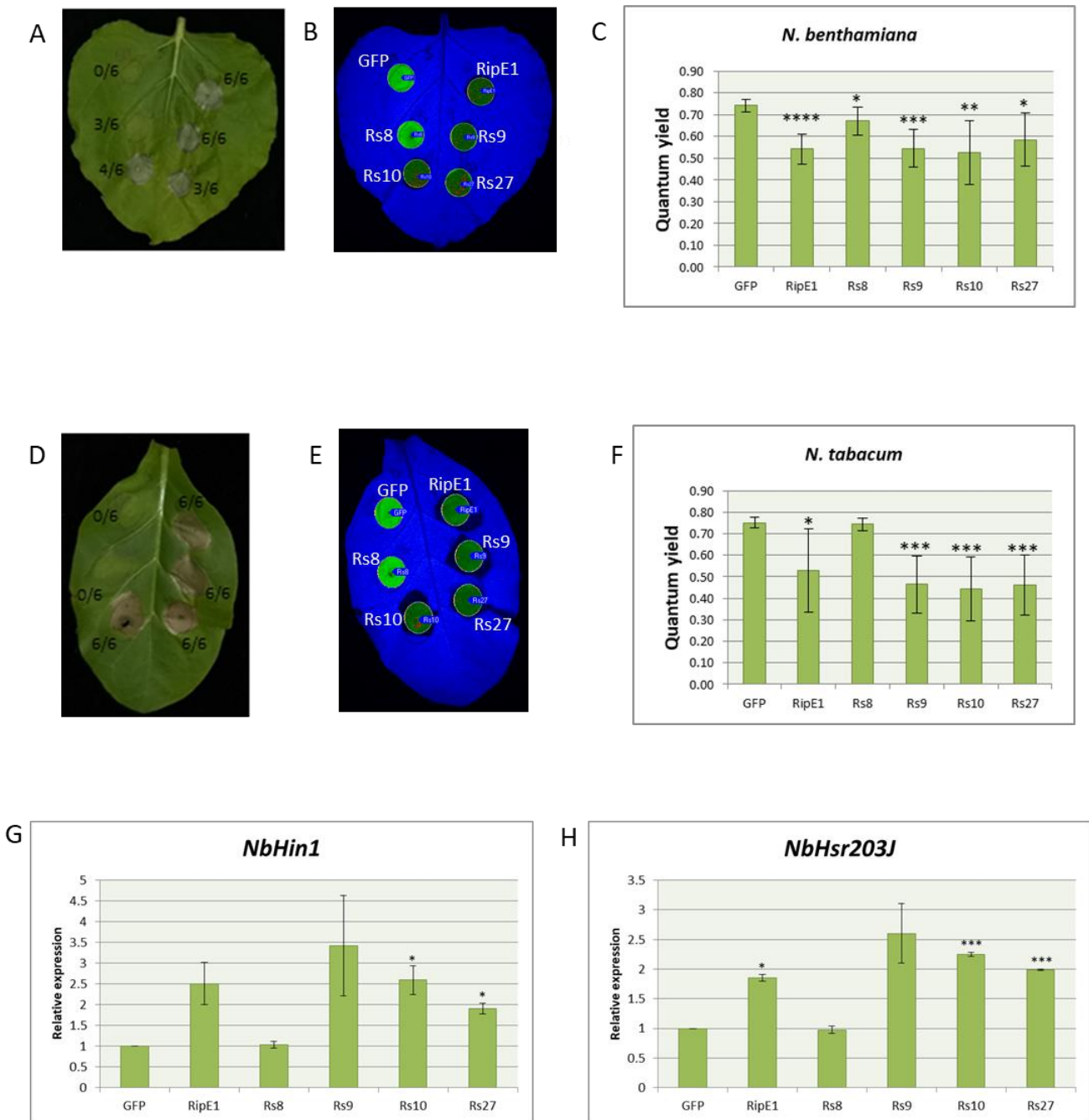


Figure 4. Several *RipB* alleles induce cell death and defense gene expression in *Nicotiana* spp.

N. benthamiana (A to C) and *N. tabacum* (D to F) were agroinfiltrated with the *RipB* alleles (*Rs8*, *Rs9*, *Rs10* and *Rs27*). Bright field and UV pictures of *N. benthamiana* (A, B) and *N. tabacum* (D, E) were taken 6 days post-infiltration. The numbers in the photographs A and D indicate the occurrence of cell death and the number of observations. The chlorophyll fluorescence parameters (C, F) were determined for each infiltration spot (n=6 repeats) Data are means of six biological repeats with error bars representing the standard error of the mean SEM. Statistical significance compared to leaf expressing GFP is indicated by asterisks (Student's t-test, $p < 0.0001$ ****, $0.0001 < p < 0.001$ ***, $0.001 < p < 0.01$ **, $0.01 < p < 0.05$ *). The ETI-marker gene *NbHIN1* (G) and *NbHsr203j* (H) expression was determined by semi-quantitative RT-PCR in similar samples as in (A) at 1 dpi. Data shown was obtained from gel quantification using ImageJ and is representative of two biological repeats.

Determination of the RipB domain required for flg22-induced ROS burst suppression and recognition in *N. benthamiana*

RipB protein sequences, including the *RipB* allele isolated from the Japanese strain (Nakano et al., 2019), were aligned using Geneious (Figure 5). Even though their protein sequences have different lengths (Rs8 393 AA, Rs9 452 AA, Rs10 518 AA and Rs27 490 AA), the alignment showed 73% of identity. It was also observed that the predicted nucleoside hydrolase domain is present in these alleles in the following positions, Rs8 137-374, Rs9 99-449, Rs10 165-515 and Rs27 137-487. However, in the alignment, it was observed that Rs9, Rs10 and Rs27 have a C-terminal extension that is absent in Rs8. Due to this major difference among the protein sequences, chimeric constructs were designed to determine if the C-terminal region plays a role for RipB suppression of flg22-triggered ROS or for the recognition of *RipB* alleles. Rs27 was chosen as representative among Rs9, Rs10 and Rs27 because their sequences are highly similar among each other (Figure 5). Chimeras were designed as: i) AE,

containing the Rs8 N-terminal and Rs27 C-terminal; ii) CB, with Rs27 N-terminal and Rs8-Cterminal; iii) D, where Rs27 C-terminal was removed; and iv) F, containing only the common sequence between Rs8 and Rs27 (Figure 6). Protein expression of chimeric constructs was confirmed by western blotting (Figure 7).

ROS burst results (Figure 8A) showed suppression of flg22-ROS production in the presence of the Rs27, but not Rs8, as previously observed (Figure 1 and 2). Chimeric construct AE (Rs8NT-Rs27CT) also suppressed flg22-ROS production. Constructs lacking the C-terminal, CB (Rs27NT-RS8CT), D (Rs27deltaCT) and F (common Rs8-Rs27), did not suppress flg22-ROS production. As observed previously (Figure 2) no significant suppression of chitin-ROS production was observed with any RipB variant (Figure 8B).

The same constructs were also tested for cell death induction, which was observed mostly in areas transiently expressing Rs27 and AE (Figure 9) in both *N. benthamiana*

and *N. tabacum*. These results suggest RipB C-terminal region is required for RipB recognition and flg22-ROS suppression.

Rs 8	-----MKAVIRSSAYSFGESGPAAT--DIDTISH-RPGPRGNM-----	36
Rs 9	-----MQARKSRPASRFPADRWKGCASPA	25
Rs 10	MI DRDHPP PSLG I TRLRP P T G P T G N S S D Y G D E G R H P I T S L S V R P T R P C H C Q D G C H N V P	60
Rs 27	-----MKAVIRSPAYPSGLR-DLAATAKT DATTY--ELRPHNSMP PGTA--	41
RS 1000	-----MP PGTA--	6
Rs 8	-----PPDASGTQKPPGKSEAGGPLEGLRKEGLGVVLPESHATHRPATEC	80
Rs 9	-----SALCS--RSTPFT-----GRPRKA	42
Rs 10	AA T T Q Q H A A R H S R R A K A A R Q V I R R R T P G T E Q D R F R --- R R A P C T I --- R T P P A G	108
Rs 27	-----GEQKPPGKSSAGGPLAGLSKTGLGVVLPESHATHRPAMES	80
RS 1000	-----GEQKPPGKSSAGGPLAGLSKTGLGVVLPESHATHRPAMES	45
Rs 8	PGAADRLLPRTRPASADAVRRALLTAFWGSHGAPEDYAEQQLLNQLRSHKPAVPMPCILF	140
Rs 9	RVPEFTASGPRTRPASADAVRRALLTAFWGSHGAPEDYAEQQLLNQLRSHKPAVPMPCILF	102
Rs 10	HGKPGRLLPRTRPASADAVRRALLTAFWGSHGAPEDYAEQQLLNQLRSHKPAVPMPCILF	168
Rs 27	LAAPARLLPRTRPASADAVRRALLTAFWGSHGAPEDYAEQQLLNQLRSHKPAVPMPCILF	140
RS 1000	LAAPARLLPRTRPASADAVRRALLTAFWGSHGAPEDYAEQQLLNQLRSHKPAVPMPCILF	105
Rs 8	TDPNKDPDDVVAFTLAKPLQVFRLVKMAHAVATLGERDVRARRAGVARGVFDRDLQEVRR	200
Rs 9	TDPNKDPDDVVAFTLAKPLQVFRLVKMAHAVATLGERDVRARRAGVARGVFDRDLQEVRR	162
Rs 10	TDPNKDPDDVVAFTLAKPLQVFRLVKMAHAVATLGERDVRARRAGVARGVFDRDLQEVRR	228
Rs 27	TDPNKDPDDVVAFTLAKPLQVFRLVKMAHAVATLGERDVRARRAGVARGVFDRDLQEVRR	200
RS 1000	TDPNKDPDDVVAFTLAKPLQVFRLVKMAHAVATLGERDVRARRAGVARGVFDRDLQEVRR	165
Rs 8	VTVGLDYAIKPEHAKDHAKFLDQGEALHVKLKPEAASEDSVAALRESLTQAAA PVTLVVI	260
Rs 9	VTVGLDYAIKPEHAKDHAKFLDQGEALHVKLKPEAASEDSVAALRESLTQAAA PVTLVVI	222
Rs 10	VTVGLDYAIKPEHAKDHAKFLDQGEALHVKLKPEAASEDSVAALRESLTQAAA PVTLVVI	288
Rs 27	VTVGLDYAIKPEHAKDHAKFLDQGEALHVKLKPEAASEDSVAALRESLTQAAA PVTLVVI	260
RS 1000	VTVGLDYAIKPEHAKDHAKFLDQGEALHVKLKPEAASEDSVAALRESLTQAAA PVTLVVI	225
Rs 8	AGMTDPCALVTAEPGLVKQKVGRVVIMGGVVRPDKDEDGYVQPPDRAYNNTTDFAAACRFY	320
Rs 9	AGMTDPCALVTAEPGLVKQKVGRVVIMGGVVRPDKDEDGYVQPPDRAYNNTTDFAAACRFY	282
Rs 10	AGMTDPCALVTAEPGLVKQKVGRVVIMGGVVRPDKDEDGYVQPPDRAYNNTTDFAAACRFY	348
Rs 27	AGMTDPCALVTAEPGLVKQKVGRVVIMGGVVRPDKDEDGYVQPPDRAYNNTTDFAAACRFY	320
RS 1000	AGMTDPCALVTAEPGLVKQKVGRVVIMGGVVRPDKDEDGYVQPPDRAYNNTTDFAAACRFY	285
Rs 8	RRVQELGI PLRI VTREAA YRAAV PRTFY EDMAQS GHVVGQYLKDVQKHALNTLWLVFKTE	380
Rs 9	RRVQELGI PLRI VTREAA YRAAV PRTFY EDMAQS GHVVGQYLKDVQKHALNTLWDGIDQG	342
Rs 10	RRVQELGI PLRI VTREAA YRAAV PRTFY EDMAQS GHVVGQYLKDVQKHALNTLWDGIDQG	408
Rs 27	RRVQELGI PLRI VTREAA YRAAV PRTFY EDMAQS GHVVGQYLKDVQKHALNTLWDGIDQG	380
RS 1000	RRVQELGI PLRI VTREAA YRAAV PRTFY EDMAQS GHVVGQYLKDVQKHALNTLWDGIDQG	345
Rs 8	ASAGSRRKV-----RNTG-----	433
Rs 9	RIAKLDKHWFNFTFIARE IGQGDAAAWAARNHTFDAIWEQVVR LNLYDPMTLLA AVPASA	402
Rs 10	RIAKLDKHWFNFTFIARE IGQGDAAAWAARNHTFDAIWEQVVR LNLYDPMTLLA AVPASA	468
Rs 27	RIAKLDKHWFNFTFIARE IGQGDAAAWAARNHTFDAIWEQVVR LNLYDPMTLLA AVPASA	440
RS 1000	RIAKLDKHWFNFTFIARE IGQGDAAAWAARNHTFDAIWEQVVR LNLYDPMTLLA AVPASA	405
Rs 8	-----	393
Rs 9	QMLFRPKAVQDAGRGLVEVIGADEVHCP SDARQLMSGLVKMALANTPGTR	452
Rs 10	QMLFRPKAVQDAGRGLVEVIGADEVHCP SDARQLMSGLVKMALANTPGTR	518
Rs 27	QMLFRPKAVQDAGRGLVEVIGADEVHCP SDARQLMSGLVKMALANTPGTR	490
RS 1000	QMLFRPKAVQDAGRGLVEVIGADEVHCP SDARQLMSGLVKMALANTPGTR	455

Figure 5. Natural variation in the *RipB* alleles sequences.

RipB protein sequences (Rs8, Rs9, Rs10, Rs27 and RS1000 from Nakano *et al.*, 2019) were aligned using Geneious program. Different amino acid residues for a given position are shown in black, deletions are indicated by a dash. Numbers show the position of the amino acid residues in each sequence.

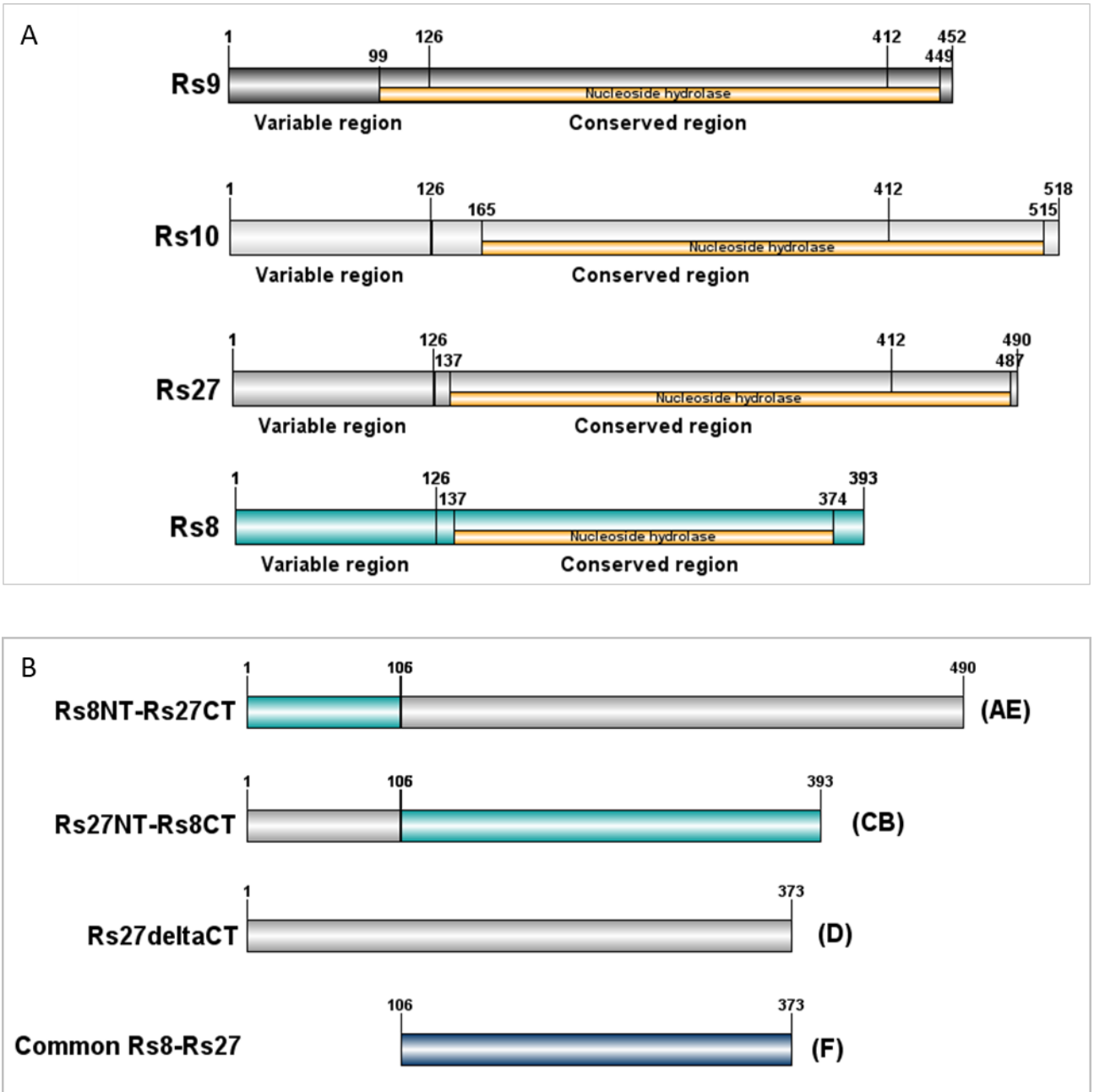


Figure 6. Schematic representation of RipB protein domains and RipB chimeric proteins.

(A) RipB proteins present in *Rso* Korean strains. The conserved nucleoside-hydrolase domain (orange) is 98.8% identical between 126 and 412. The N-terminal region is termed variable as the 12.7% of identity varies between 1 and 126. (B) RipB chimeric proteins obtained in this study. AE, containing the Rs8 N-terminal and Rs27 C-terminal; CB, with Rs27 N-terminal and Rs8-C-terminal; D, where Rs27 C-terminal was removed; and F, containing only the common sequence between Rs8 and Rs27. Numbers indicate amino acid positions. AE, CB, D and F represent abbreviations of the chimeric constructs.

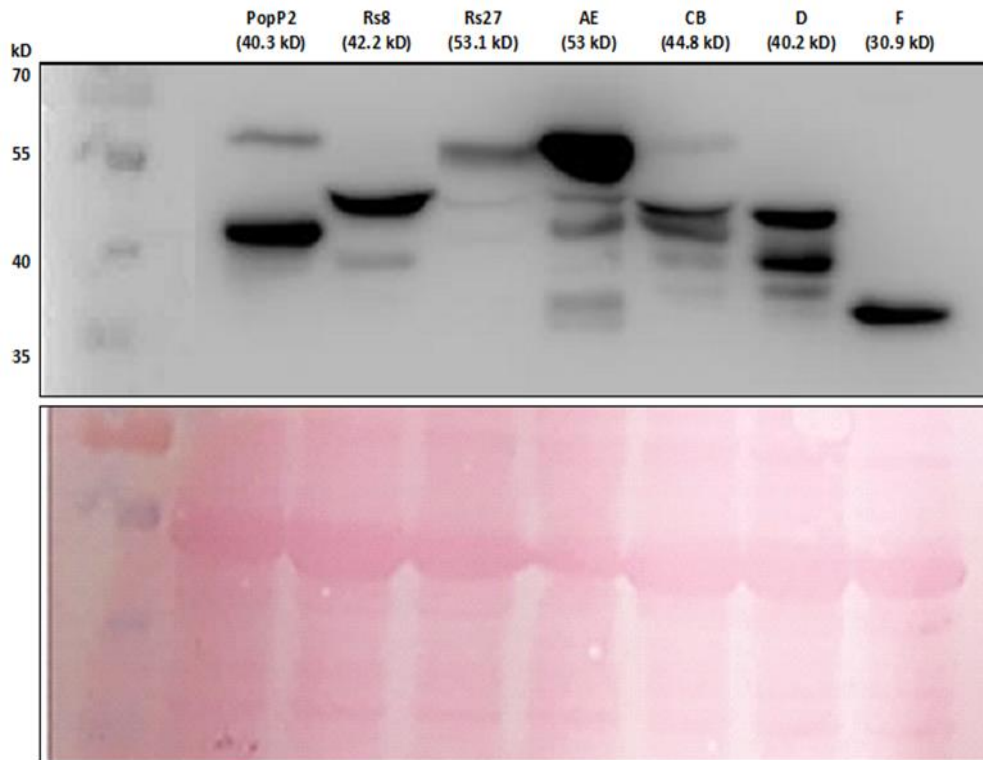


Figure 7. Expression of RipB chimeric constructs in *N. benthamiana*.

Rs8, *Rs27* and chimeric constructs were agroinfiltrated in *N. benthamiana* and harvested 2 days post-infiltration. Western blot with anti-flag antibody show *Rs8*, *Rs27*, AE, CB, D and F (top panel). Membrane was stained with Ponceau S (bottom panel). Ladder is shown on the left. Predicted molecular weights are below the sample names. PopP2-3xFLAG was included as control. AE: *Rs8NT-Rs27CT*, CB: *Rs27NT-Rs8CT*, D: *Rs27deltaCT* and F: Common *Rs8-Rs27*.

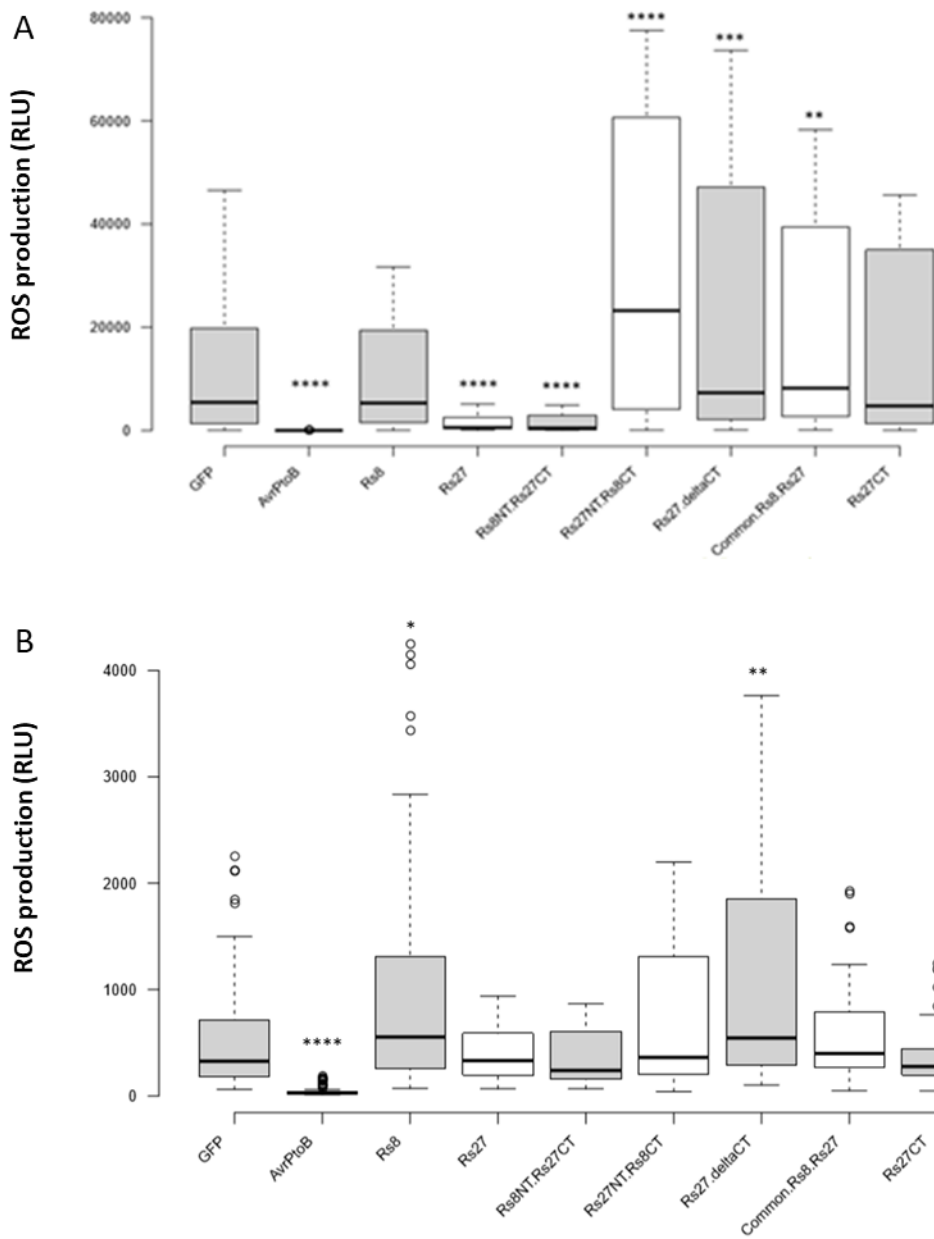


Figure 8. RipB C-terminal region is necessary for flg22-ROS burst suppression in *N. benthamiana*. ROS burst was elicited by 50 nM flg22 (A) or 100 µg/ml chitin (B) in *N. benthamiana* transiently expressing the Rs8, Rs27 or chimeric constructs. GFP was used as a positive control and AvrPtoB as a negative control. Data are means of three biological repeats with error bars representing the SEM (n=18 for effectors and n=48 for GFP and AvrPtoB). Statistical significance compared to leaf expressing GFP is indicated by asterisks (Student's t-test, $p < 0.0001$ ****, $0.0001 < p < 0.001$ ***, $0.001 < p < 0.01$ **, $0.01 < p < 0.05$ *).

Roq1 silencing in *N. benthamiana* to assess if Roq1 recognition of RipB effectors is the reason for ROS burst suppression

RipB shares close homology with *Xanthomonas* effector protein XopQ, which is recognized by the NLR protein Roq1 from *N. benthamiana* (Nakano et al., 2019; Schiltink et al., 2017). To test if Roq1 was involved in RipB recognition, *Roq1* expression in *N. benthamiana* was silenced (TRV:Roq1) using VIGS system (Figure 10). Silencing of *Roq1* did not affect plant morphology or development. It was demonstrated by RT-PCR that *Roq1* expression was reduced by approximately 54% in pTRV2:Roq1 plants compared with pTRV2:EV.

To evaluate if RipB recognition by Roq1 is associated with cell death, TRV:Roq1 and TRV:EV leaves were agroinfiltrated with Rs8 and Rs27 (GFP and RipE1 were used as positive and negative controls, respectively) and chlorophyll fluorescence kinetics for each area was measured at 6 dpi (Figure 11). Cell death was observed only in Rs27 infiltrated spots in TRV:EV

plants (Figure 10 A-C), but no cell death was observed in *Roq1* silenced plants (Figure 10 D-F). These results indicate that *Roq1* is involved in *RipB* recognition leading to cell death due to the C-terminal present in Rs27.

Then the next question was if *RipB* could suppress PTI when it is not recognized. To assess if *Roq1* was linked with flg22- and chitin- ROS suppression by *RipB*, ROS burst was measured in TRV:Roq1 and TRV:EV leaf discs transiently expressing *RipB* alleles (Figure 12). Results showed a significant reduction in flg22-ROS production when Rs27 and AE were expressed, in both, TRV:Roq1 and TRV:EV plants (Figure 13A). Conversely to previous results observed in wild-type *N. benthamiana* (Figure 2 and Figure 8), chitin-ROS production was significantly suppressed in presence of Rs27 and AE, in both, TRV:Roq1 and TRV:EV (Figure 12B). Constitutive ROS did not present significant differences between TRV:Roq1 and TRV:EV plants (Figure 12C). Reduction of *Roq1* expression was confirmed by qPCR (Figure 12D). Together these results suggest

that flg22-ROS burst might not be linked with RipB recognition by Roq1, but with RipB virulence activity.

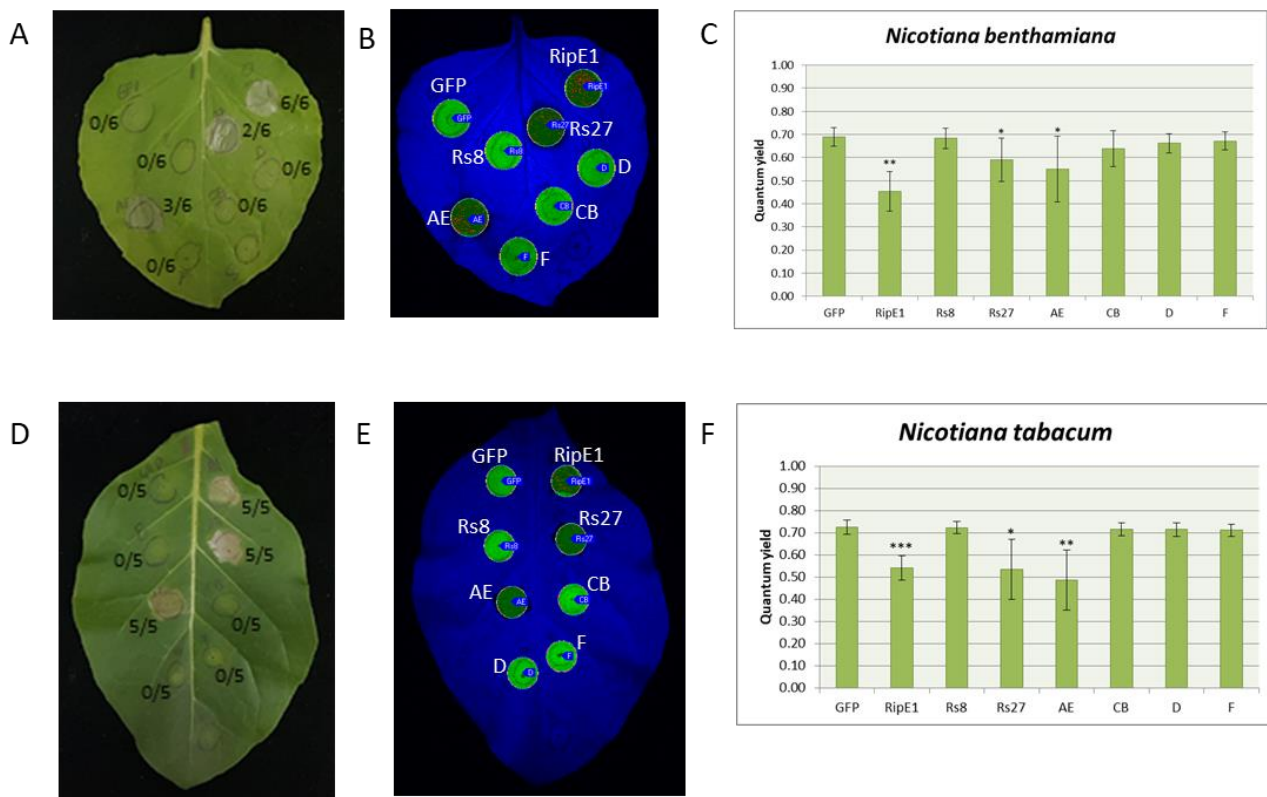


Figure 9. RipB's C-terminal is required for the induction of cell death in *Nicotiana spp.*

Nicotiana benthamiana (A to C) and *Nicotiana tabacum* (D to F) were agroinfiltrated with the *RipB* alleles (*Rs8*, *Rs27*) and chimeric constructs. Bright field and UV pictures of *N. benthamiana* (A, B) and *N. tabacum* (D, E) were taken 6 days post-infiltration and the chlorophyll fluorescence parameters (C, F) determined for each infiltration spot A and D. The numbers in the photograph indicate the ratios of infiltration showing cell death to total number of infiltrations. Statistical significance compared to leaf expressing GFP is indicated by asterisks (Student's t-test, $p < 0.0001$ ****, $0.0001 < p < 0.001$ ***, $0.001 < p < 0.01$ **, $0.01 < p < 0.05$ *). AE: Rs8NT-Rs27CT, CB: Rs27NT-Rs8CT, D: Rs27deltaCT and F: Common Rs8-Rs27.

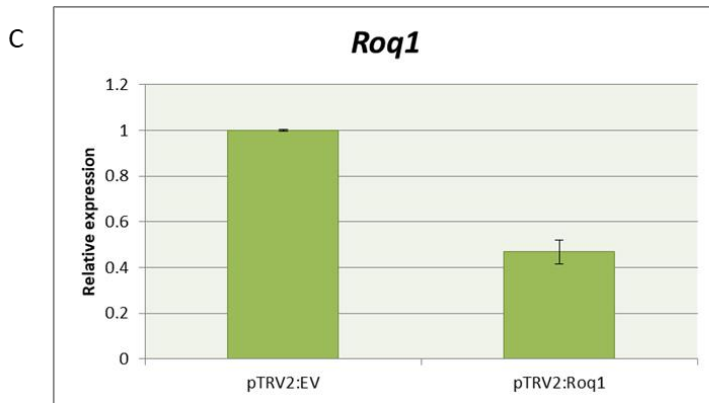
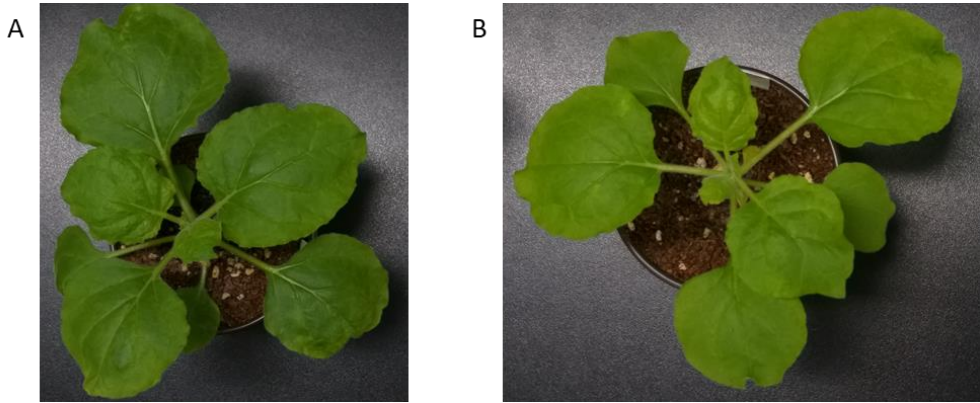


Figure 10. Characterization of Roq1-silenced plants.

Picture of *N. benthamiana* plant 4 weeks after infiltration with pTRV:EV (A) or pTRV2:Roq1 (B). (C) *Roq1* expression was determined by qPCR, normalized by *NbEF1a* and is shown relative to TRV:EV plants.

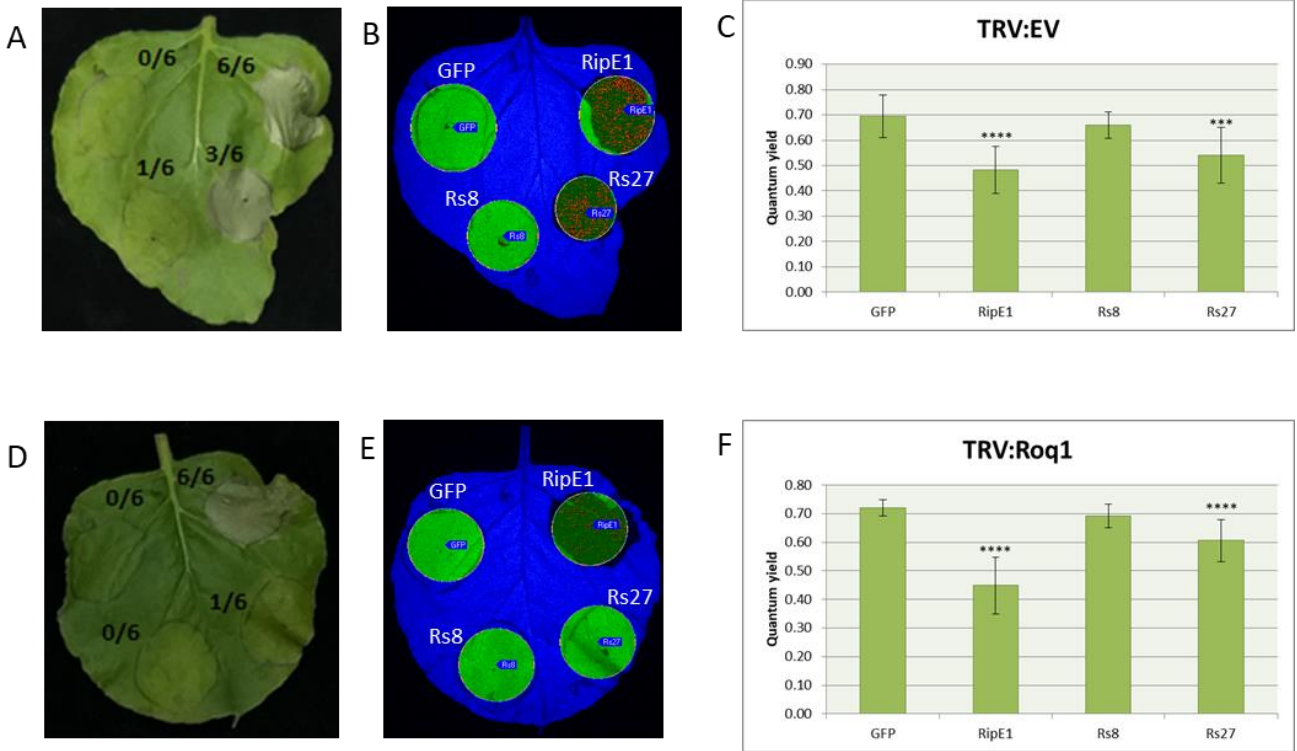


Figure 11. *Roq1* might be involved in recognition of RipB C-terminal region leading to cell death.

Nicotiana benthamiana plants infiltrated with TRV:EV (A to C) and TRV:Roq1 (D to F) were agroinfiltrated with the *RipB* alleles (*Rs8*, *Rs27*). Bright field (A, D) and UV (B, E) pictures were taken 6 days post-infiltration and the chlorophyll fluorescence parameters (C, F) determined for each infiltration spot. A and D. The numbers in the photograph indicate the ratios of infiltration showing cell death to total number of infiltrations. Statistical significance compared to leaf expressing GFP is indicated by asterisks (Student's t-test, $p < 0.0001$ ****, $0.0001 < p < 0.001$ ***, $0.001 < p < 0.01$ **, $0.01 < p < 0.05$ *).

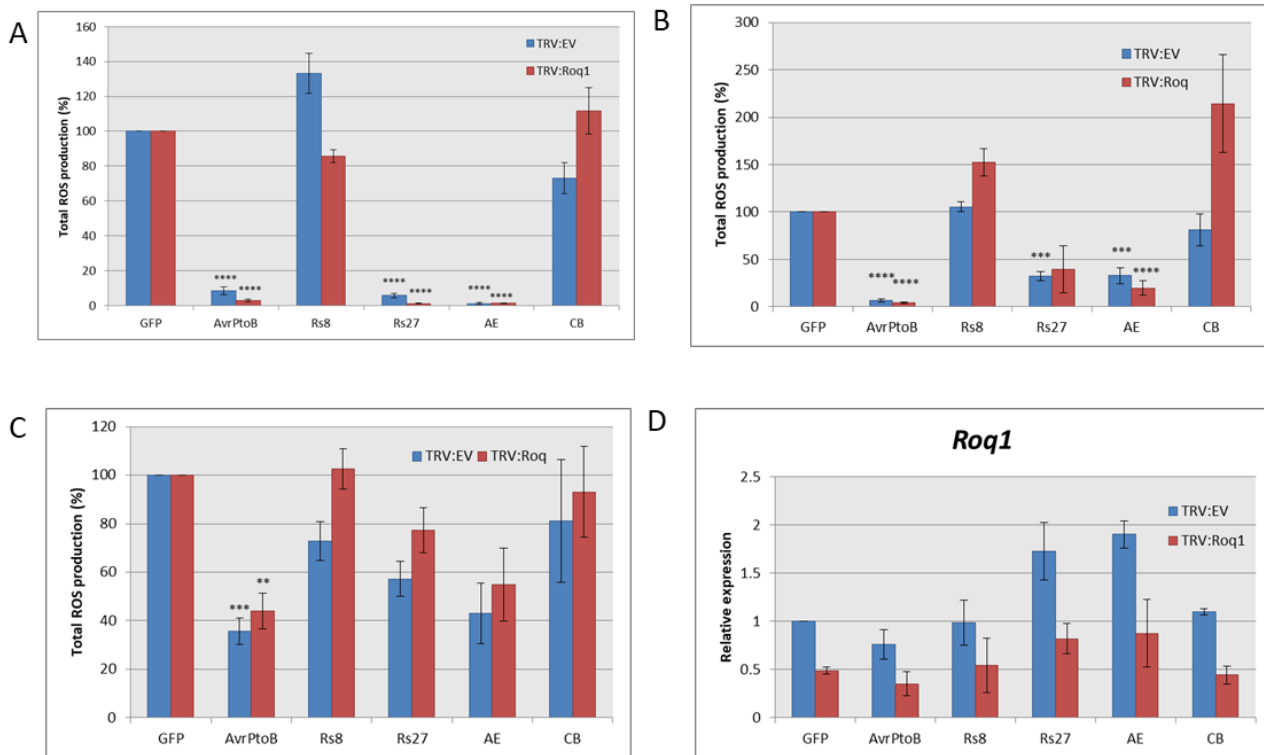


Figure 12. RipB suppression of ROS burst might not be linked with RipB recognition by Roq1.

ROS burst was elicited by 50 nM flg22 (A), 100 ug/ml chitin (B) or water (C) in *Roq1*-silenced *N. benthamiana* transiently expressing the *RipB* alleles (*Rs8* and *Rs27*) and two chimeric constructs (AE and CB). GFP and AvrPtoB were used as positive and negative controls respectively. Data are means of three biological repeats with error bars representing the SEM (n=40 or n=48 for *RipB* alleles, GFP and AvrPtoB, and n=24 for chimeric constructs). Statistical significance compared to leaf expressing GFP is indicated by asterisks ((Student's t-test, $p < 0.0001$ ****, $0.0001 < p < 0.001$ ***, $0.001 < p < 0.01$ **, $0.01 < p < 0.05$ *). D. *Roq1* expression was determined by qPCR and normalized by *NbEF1a*. AE: Rs8NT-Rs27CT, CB: Rs27NT-Rs8CT

DISCUSSION

Ralstonia solanacearum relies on the type III secretion system for its pathogenicity, which injects type III effector proteins into plant cells that collectively modulate plant immunity (Galán et al., 2014; Büttner, 2016).

Various pathogen-related molecules, referred as elicitors, directly trigger the oxidative burst, and other defense responses (Averyanov, 2009). In this study individual effectors cloned from *Rso* strains collected across South Korea were screened to assess their effect in plant immunity responses. Flg22-triggered ROS production was differently modulated by the agroinfiltrated effectors. In accordance with my results, Korean alleles of *RipAY* (Sang et al., 2018) and *RipAC* (Yu et al., 2020) were reported to suppress PAMP-triggered ROS burst. This ROS burst suppression might be a mechanism of suppression of the defense responses in plants.

To understand *RipB* virulence function I looked at flg22 and chitin ROS burst. None of *RipB* alleles induced a significant constitutive ROS production. In previous studies *RipB* (RS1000) was

found to lead to constitutive ROS production (Nakano et al., 2019). On the other hand, Rs9, Rs10 and Rs27 significantly reduced flg22-triggered ROS, but Rs8 did not show a significant reduction (compared to GFP), while chitin-triggered ROS burst did not present significant changes. This might indicate that Rs9, Rs10 and Rs27 modulate flg22-ROS but not chitin-ROS burst. Interestingly, RipB homolog from *Pseudomonas syringae* HopQ1 directly affects flg22 but not chitin responses in *Arabidopsis* (Hann et al., 2014).

It is important to consider that RipB_RS1000 was obtained from a Japanese Rso strain while ours were isolated from Korean strains, and protein alignment showed differences between the effectors used in both studies. Furthermore, it is possible that the difference in ROS burst could be due to sequence variation among *RipB* alleles (*Rs8*, *Rs9*, *Rs10* and *Rs27*), and flg22-ROS suppression could be the result of RipB virulence activity to suppress plant defense.

Predicted effector sequences of RipB from Rso Korean strains were analyzed for known protein domains, showing that RipB is predicted to carry a nucleoside-hydrolase (NH) domain, consistent

with previous predictions (Peeters et al., 2013). This domain is similar to the one present in HopQ1 and XopQ (Hann *et al.*, 2014; Schultink *et al.*, 2017). Additionally, it has been reported that HopQ1 promotes bacterial virulence dependent on its NH domain, and that there is a conserved aspartate motif, representing the nucleoside binding site (Hann *et al.*, 2014).

Protein alignment showed that there is variation among *RipB* alleles where the C-terminal is absent in Rs8. This region contains a catalytic pocket from the NH domain, hence lacking the conserved aspartate residue. This suggests that a full length NH domain is required for RipB virulence activity.

Following this hypothesis, chimeric constructs were tested. A strong reduction of flg22-triggered ROS burst was only observed in areas infiltrated with Rs27 and AE (Rs8NT-Rs27CT) construct. However no significant modulation was observed in chitin-triggered ROS, compared to GFP. These results confirm the importance of the C-terminal region for RipB activity. This was also found by Nakano *et*

al., 2019, where it was shown that deletion of C-terminal abolished RipB ability to induce constitutive ROS production in *N. benthamiana*.

We also found Rs9, Rs10 and Rs27 but not Rs8 triggered cell death in *N. benthamiana*, and induced expression of ETI-marker genes *NbHin1* and *NbHsr203J*. This is similar to RS1000 RipB, which triggers constitutive ROS production and induces *NbHin1* expression although no cell death was observed. Furthermore, cell death was not induced in spots infiltrated with CB (Rs27NT-Rs8CT) construct. These findings support the requirement of a functional NH domain for RipB virulence activity. It is worth mentioning that cell death was not observed in all the infiltrated spots in a reproducible manner. This might be due to the expression vector and the strong promoter 35S used, as well as to our experimental conditions, yet controlled, did not guarantee the plants being at the exact same state. Nonetheless, together, Nakano *et al.*, and my data indicate that cell death induced by RipB is likely the result of the recognition of RipB by a NLR gene in *N. benthamiana*.

The NLR protein Roq1 recognizes HopQ1 and XopQ (Schultink *et al.*, 2017), both close homologues of RipB, therefore it is possible that Roq1 also recognizes RipB. It has been reported that *Rso* strain carrying only RipB can grow and induce disease in *Roq1* silenced *N. benthamiana*, but not in wild-type *N. benthamiana*, indicating that RipB is a major avirulence factor recognized by Roq1 (Nakano *et al.*, 2019). We hypothesized that the suppression of flg22-ROS burst could be the result of the ETI response ongoing in cells expressing RipB, so we measured flg22-ROS burst in Roq1 silenced *N. benthamiana*.

An inconvenient of VIGS is that the silencing efficiency might be low and not uniform (Senthil-Kumar and Mysore, 2014). Consequently, although *Roq1* expression was reduced, it was not constantly reduced among the silenced plants. Although Roq1 silencing did reduce the frequency of cell death induced by Rs27, it would be proper to use stable *Roq1* knock-out plants, generated using CRISPR/Cas9 technique for example, to confirm that RipB is indeed recognized by Roq1 in *N. benthamiana*. Furthermore, analyzing flg22-

and chitin-triggered ROS burst in *Roq1* silenced *N. benthamiana*, I found no significant difference compared with the plants carrying an empty vector, indicating that flg22-ROS suppression might be related to RipB virulence rather than to ETI activation.

REFERENCES

- Averyanov A. (2009). Oxidative burst and plant disease resistance. *Frontiers in bioscience (Elite edition)*, 1, 142–152.
- Bai, C., Sen, P., Hofmann, K., Ma, L., Goebel, M., Harper, J. W., & Elledge, S. J. (1996). SKP1 connects cell cycle regulators to the ubiquitin proteolysis machinery through a novel motif, the F-box. *Cell*, 86, 263–274.
- Bai, J., Choi, S. H., Ponciano, G., Leung, H., & Leach, J. E. (2000). *Xanthomonas oryzae* pv. *oryzae* avirulence genes contribute differently and specifically to pathogen aggressiveness. *Molecular plant-microbe interactions* : MPMI, 13, 1322–1329.
- Baker, C. J., & Orlandi, E. W. (1995). Active oxygen in plant pathogenesis. *Annual Review of Phytopathology*, 33, 299–321.
- Bally, J., Jung, H., Mortimer, C., Naim, F., Philips, J. G., Hellens, R., ... Waterhouse, P. M. (2018). The Rise and Rise of *Nicotiana benthamiana*: A Plant for All Reasons. *Annual*

Review of Phytopathology, 56, 405–426.

Baruch, K., Gur-Arie, L., Nadler, C., Koby, S., Yerushalmi, G., Ben-Neriah, Y., Yogev, O., Shaulian, E., Guttman, C., Zarivach, R., & Rosenshine, I. (2011). Metalloprotease type III effectors that specifically cleave JNK and NF- κ B. *The EMBO journal*, 30, 221–231.
<https://doi.org/10.1038/emboj.2010.297>

Boller, T., & Felix, G. (2009). A renaissance of elicitors: Perception of microbe-associated molecular patterns and danger signals by pattern-recognition receptors. *Annual Review of Plant Biology*, 60, 379–406.

Boutrot, F., & Zipfel, C. (2017). Function, discovery, and exploitation of plant pattern recognition receptors for broad-spectrum disease resistance. *Annual Review of Phytopathology*, 55, 11.1-11.30.

Büttner, D. (2016). Behind the lines-actions of bacterial type III effector proteins in plant cells. *FEMS Microbiology Reviews*,

40, 894–937.

Chinchilla, D., Bauer, Z., Regenass, M., Boller, T., & Felix, G. (2006). The *Arabidopsis* receptor kinase FLS2 binds flg22 and determines the specificity of flagellin perception. *The Plant cell*, 18, 465–476.

Chisholm, S. T., Coaker, G., Day, B., & Staskawicz, B. J. (2006). Host-microbe interactions: shaping the evolution of the plant immune response. *Cell*, 124, 803–814.

Chiu, W., Niwa, Y., Zeng, W., Hirano, T., Kobayashi, H., & Sheen, J. (1996). Engineered GFP as a vital reporter in plants. *Current biology : CB*, 6, 325–330.

Couto, D., & Zipfel, C. (2016). Regulation of pattern recognition receptor signalling in plants. *Macmillan Publishers*, 16, 537–552.

Cui, H., Tsuda, K., & Parker, J. E. (2015). Effector-triggered immunity: From pathogen perception to robust defense. *Annual Review of Plant Biology*, 66, 487–551.

- Deslandes, L., & Rivas, S. (2012). Catch me if you can: Bacterial effectors and plant targets. *Trends in Plant Science*, *17*, 644–655.
- Degano, M., Gopaul, D. N., Scapin, G., Schramm, V. L., & Sacchettini, J. C. (1996). Three-dimensional structure of the inosine-uridine nucleoside N-ribohydrolase from *Crithidia fasciculata*. *Biochemistry*, *35*, 5971–5981.
- Dodds, P. N., & Rathjen, J. P. (2010). Plant immunity: Towards an integrated view of plant-pathogen interactions. *Nature Reviews Genetics*, *11*, 539–548.
- Fujiwara, S., Kawazoe, T., Ohnishi, K., Kitagawa, T., Popa, C., Valls, M., ... Tabuchi, M. (2016). RipAY, a plant pathogen effector protein, exhibits robust γ -Glutamyl Cyclotransferase activity when stimulated by eukaryotic thioredoxins. *Journal of Biological Chemistry*, *291*, 6813–6830.
- Galán, J. E., Lara-Tejero, M., Marlovits, T. C., & Wagner, S. (2014). Bacterial type III secretion systems: specialized

nanomachines for protein delivery into target cells. *Annual review of microbiology*, 68, 415–438.

Gimenez-Ibanez, S., Hann, D. R., Ntoukakis, V., Petutschnig, E., Lipka, V., & Rathjen, J. P. (2009). AvrPtoB targets the LysM receptor kinase CERK1 to promote bacterial virulence on plants. *Current Biology*, 19, 423–429.

Gimenez-Ibanez, S., Hann, D. R., Chang, J. H., Segonzac, C., Boller, T., & Rathjen, J. P. (2018). Differential Suppression of *Nicotiana benthamiana* Innate Immune Responses by Transiently Expressed *Pseudomonas syringae* Type III Effectors. *Frontiers in plant science*, 9, 1-19.

Gopalan, S., Wei, W., & He, S. Y. (1996). hrp gene-dependent induction of *hin1*: a plant gene activated rapidly by both harpins and the avrPto gene-mediated signal. *The Plant journal : for cell and molecular biology*, 10, 591–600.

Hahlbrock, K., Bednarek, P., Ciolkowski, I., Hamberger, B., Heise, A., Liedgens, H., Logemann, E., Nürnberger, T.,

Schmelzer, E., Somssich, I. E., & Tan, J. (2003). Non-self recognition, transcriptional reprogramming, and secondary metabolite accumulation during plant/pathogen interactions. *Proceedings of the National Academy of Sciences of the United States of America*, 100 Suppl 2, 14569–14576.

Hann, D. R., Domínguez-Ferreras, A., Motyka, V., Dobrev, P. I., Schornack, S., Jehle, A., ... Boller, T. (2014). The *Pseudomonas* type III effector HopQ1 activates cytokinin signaling and interferes with plant innate immunity. *New Phytologist*, 201(2), 585–598.

Hisano, T., Hata, Y., Fujii, T., Liu, J. Q., Kurihara, T., Esaki, N., & Soda, K. (1996). Crystal structure of L-2-haloacid dehalogenase from *Pseudomonas* sp. YL. An alpha/beta hydrolase structure that is different from the alpha/beta hydrolase fold. *The Journal of biological chemistry*, 271, 20322–20330.

Holmes, E. C., Chen, Y. C., Sattely, E. S., & Mudgett, M. B.

(2019). An engineered pathway for N-hydroxy-pipecolic acid synthesis enhances systemic acquired resistance in tomato. *Science Signaling*, *12*, 1–10.

Jacob, F., Vernaldi, S., & Maekawa, T. (2013). Evolution and conservation of plant NLR functions. *Frontiers in Immunology*, *4*, 1–16.

Jones, J. D. G., & Dangl, J. L. (2006). The plant immune system. *Nature*, *444*, 323–329.

Jwa, N. S., & Hwang, B. K. (2017). Convergent evolution of pathogen effectors toward reactive oxygen species signaling networks in plants. *Frontiers in Plant Science*, *8*, 1–12.

Karuppanan, K., Duhra-Gill, S., Kailemia, M. J., Phu, M. L., Lebrilla, C. B., Dandekar, A. M., ... McDonald, K. A. (2017). Expression, purification, and biophysical characterization of a secreted anthrax decoy fusion protein in *Nicotiana benthamiana*. *International Journal of Molecular Sciences*, *18*, 1–13.

Katagiri, F., Thilmony, R., & He, S. Y. (2002). The *Arabidopsis thaliana-pseudomonas syringae* interaction. *The arabidopsis book*, 1, 1-35.

Kim, W., Prokchorchik, M., Tian, Y., Kim, S., Jeon, H., & Segonzac, C. (2020). Perception of unrelated microbe-associated molecular patterns triggers conserved yet variable physiological and transcriptional changes in *Brassica rapa* ssp. *pekinensis*. *Horticulture Research*, 7, 1–12.

Kirigia, D., Runo, S., & Alakonya, A. (2014). A virus-induced gene silencing (VIGS) system for functional genomics in the parasitic plant *Striga hermonthica*. *Plant Methods*, 10, 1–8.

Künstler, A., Bacsó, R., Gullner, G., Hafez, Y. M., & Király, L. (2016). Staying alive - is cell death dispensable for plant disease resistance during the hypersensitive response? *Physiological and Molecular Plant Pathology*, 93, 75–84.

Kunze, G., Zipfel, C., Robatzek, S., Niehaus, K., Boller, T., & Felix, G. (2004). The N terminus of bacterial elongation

factor Tu elicits innate immunity in *Arabidopsis* plants. *The Plant cell*, 16, 3496–3507.

Li, Q., Ai, G., Shen, D., Zou, F., Wang, J., Bai, T., ... Dou, D. (2019). A *Phytophthora capsici* effector targets ACD11 binding partners that regulate ROS-mediated defense response in *Arabidopsis*. *Molecular Plant*, 12, 565–581.

Lomax, J. E., Bianchetti, C. M., Chang, A., Phillips, G. N., Jr, Fox, B. G., & Raines, R. T. (2014). Functional evolution of ribonuclease inhibitor: insights from birds and reptiles. *Journal of molecular biology*, 426, 3041–3056.

Lowe-Power, T. M., Khokhani, D., & Allen, C. (2018). How *Ralstonia solanacearum* Exploits and Thrives in the Flowing Plant Xylem Environment. *Trends in microbiology*, 26, 929–942.

Macho, A. P. (2016). Subversion of plant cellular functions by bacterial type-III effectors: Beyond suppression of immunity. *New Phytologist*, 210, 51–57.

Macho, A. P., & Zipfel, C. (2014). Plant PRRs and the activation of innate immune signaling. *Molecular cell*, 54, 263–272.

Mak, A. N., Bradley, P., Cernadas, R. A., Bogdanove, A. J., & Stoddard, B. L. (2012). The crystal structure of TAL effector PthXo1 bound to its DNA target. *Science (New York, N.Y.)*, 335, 716–719.

Matsunaga, W., Shimura, H., Shirakawa, S., Isoda, R., Inukai, T., Matsumura, T., & Masuta, C. (2019). Transcriptional silencing of 35S driven-transgene is differentially determined depending on promoter methylation heterogeneity at specific cytosines in both plus- and minus-sense strands. *BMC Plant Biology*, 19, 1–13

McLennan A. G. (2006). The Nudix hydrolase superfamily. *Cellular and molecular life sciences : CMLS*, 63, 123–143.

Mhamdi, A., & Van Breusegem, F. (2018). Reactive oxygen species in plant development. *Annual Review of Phytopathology*, 69, 209–236.

- Miller, G., Schlauch, K., Tam, R., Cortes, D., Torres, M. A., Shulaev, V., ... Mittler, R. (2010). The Plant NADPH Oxidase RBOHD Mediates Rapid Systemic Signaling in Response to Diverse Stimuli. *Plant Biology*, 2, 1–10.
- Mittler, R. (2017). ROS are good. *Trends in Plant Science*, 22, 11–19.
- Moore, J. W., Loake, G. J., & Spoel, S. H. (2011). Transcription dynamics in plant immunity. *Plant Cell*, 23, 2809–2820.
- Mukaihara, T., Hatanaka, T., Nakano, M., & Oda, K. (2016). *Ralstonia solanacearum* type III Effector RipAY is a glutathione- degrading enzyme that is activated by plant cytosolic thioredoxins and suppresses plant immunity. *MBio*, 7, 1–16.
- Mukaihara, T., Tamura, N., Murata, Y., & Iwabuchi, M. (2004). Genetic screening of Hrp type III-related pathogenicity genes controlled by the HrpB transcriptional activator in *Ralstonia solanacearum*. *Molecular Microbiology*, 54, 863–875.

Nakano, M., & Mukaihara, T. (2019). The type III effector RipB from *Ralstonia solanacearum* RS1000 acts as a major avirulence factor in *Nicotiana benthamiana* and other *Nicotiana* species. *Molecular Plant Pathology*, 20, 1237–1251.

Nicaise, V., Roux, M., & Zipfel, C. (2009). Recent advances in PAMP-Triggered Immunity against bacteria: Pattern Recognition Receptors watch over and raise the alarm. *Plant Physiology*, 150, 1638–1647.

Oakley, A. J., Yamada, T., Liu, D., Coggan, M., Clark, A. G., & Board, P. G. (2008). The identification and structural characterization of C7orf24 as gamma-glutamyl cyclotransferase. An essential enzyme in the gamma-glutamyl cycle. *The Journal of biological chemistry*, 283, 22031–22042.

Peeters, N., Carrère, S., Anisimova, M., Plener, L., Cazalé, A. C., & Genin, S. (2013). Répertoire, unified nomenclature and

evolution of the Type III effector gene set in the *Ralstonia solanacearum* species complex. *BMC Genomics*, *14*, 1–18.

Peeters, N., Guidot, A., Vailleau, F., & Valls, M. (2013). *Ralstonia solanacearum*, a widespread bacterial plant pathogen in the post-genomic era. *Molecular Plant Pathology*, *14*, 651–662.

Perrier, A., Barlet, X., Rengel, D., Prior, P., Poussier, S., Genin, S., & Guidot, A. (2019). Spontaneous mutations in a regulatory gene induce phenotypic heterogeneity and adaptation of *Ralstonia solanacearum* to changing environments. *Scientific reports*, *21*, 3140–3152.

Pontier, D., Godiard, L., Marco, Y., & Roby, D. (1994). *hsr203J*, a tobacco gene whose activation is rapid, highly localized and specific for incompatible plant/pathogen interactions. *The Plant journal : for cell and molecular biology*, *5*, 507–521.

Prokhorchik, M., Choi, S., Chung, E.-H., Won, K., Dangl, J.L. and Sohn, K.H. (2020), A host target of a bacterial cysteine

- protease virulence effector plays a key role in convergent evolution of plant innate immune system receptors. *New Phytol*, 225: 1327-1342. Qi, J., Wang, J., Gong, Z., & Zhou, J. M. (2017). Apoplastic ROS signaling in plant immunity. *Current Opinion in Plant Biology*, 38, 92–100.
- Ramegowda, V., Mysore, K. S., & Senthil-Kumar, M. (2014). Virus-induced gene silencing is a versatile tool for unraveling the functional relevance of multiple abiotic-stress-responsive genes in crop plants. *Frontiers in Plant Science*, 5, 1–12.
- Ranf, S. (2018). Pattern Recognition Receptors — Versatile Genetic Tools for Engineering Broad-Spectrum Disease Resistance in Crops. *MDPI*, 8, 1–13.
- Sang, Y., Wang, Y., Ni, H., Cazalé, A. C., She, Y. M., Peeters, N., & Macho, A. P. (2018). The *ralstonia solanacearum* type III effector *ripay* targets plant redox regulators to suppress immune responses. *Molecular Plant Pathology*, 19, 129–142.
- Sang, Y., Yu, W., Zhuang, H., Wei, Y., Derevnina, L., Yu, G.,

- Luo, J., & Macho, A. P. (2020). Intra-strain Elicitation and Suppression of Plant Immunity by *Ralstonia solanacearum* Type-III Effectors in *Nicotiana benthamiana*. *Plant communications*, 1, 1-14.
- Schultink, A., Qi, T., Lee, A., Steinbrenner, A. D., & Staskawicz, B. (2017). Roq1 mediates recognition of the *Xanthomonas* and *Pseudomonas* effector proteins XopQ and HopQ1. *The Plant Journal*, 92, 787–795.
- Segonzac, C., Feike, D., Gimenez-Ibanez, S., Hann, D. R., Zipfel, C., & Rathjen, J. P. (2011). Hierarchy and roles of pathogen-associated molecular pattern-induced responses in *Nicotiana benthamiana*. *Plant Physiology*, 156, 687–699.
- Segonzac, C., Newman, T. E., Choi, S., Jayaraman, J., Choi, D. S., Jung, G. Y., Cho, H., Lee, Y. K., & Sohn, K. H. (2017). A Conserved EAR Motif Is Required for Avirulence and Stability of the *Ralstonia solanacearum* Effector PopP2 In *Planta*. *Frontiers in plant science*, 8, 1- 13.

- Segonzac, C., & Zipfel, C. (2011). Activation of plant pattern-recognition receptors by bacteria. *Current Opinion in Microbiology*, *14*, 54–61.
- Senthil-Kumar, M., & Mysore, K. S. (2014). Tobacco rattle virus-based virus-induced gene silencing in *Nicotiana benthamiana*. *Nature*, *9*, 1549–1562.
- Sun, Y., Li, P., Shen, D., Wei, Q., He, J., & Lu, Y. (2019). The *Ralstonia solanacearum* effector RipN suppresses plant PAMP-triggered immunity, localizes to the endoplasmic reticulum and nucleus, and alters the NADH/NAD⁺ ratio in *Arabidopsis*. *Molecular Plant Pathology*, *20*, 533–546.
- Tameling, W. I. L., & Takken, F. L. W. (2008). Resistance proteins: Scouts of the plant innate immune system. *European Journal of Plant Pathology*, *121*, 243–255.
- Unver, T., & Budak, H. (2009). Virus-induced gene silencing, A post transcriptional gene silencing method. *International Journal of Plant Genomics*, *2009*, 1–8.

- van der Burgh, A. M., & Joosten, M. H. A. J. (2019). Plant Immunity: Thinking Outside and Inside the Box. *Trends in Plant Science*, 24, 587–601.
- Wang, Y., & Ng, T. Y. (2006). Phosphatase 2A negatively regulates mitotic exit in *Saccharomyces cerevisiae*. *Molecular biology of the cell*, 17, 80–89.
- Wang, K., Uppalapati, S. R., Zhu, X., Dinesh-Kumar, S. P., & Mysore, K. S. (2010). SGT1 positively regulates the process of plant cell death during both compatible and incompatible plant-pathogen interactions. *Molecular Plant Pathology*, 11, 597–611.
- Wu, Y., Zhang, D., Chu, J. Y., Boyle, P., Wang, Y., Brindle, I. D., ... Després, C. (2012). The *Arabidopsis* NPR1 protein is a receptor for the plant defense hormone salicylic acid. *Cell Reports*, 1, 639–647.
- Yang, G., Sau, C., Lai, W., Cichon, J., & Li, W. (2015). Bacterial type III secretion systems: specialized nanomachines for

protein delivery into target cells. *Annual Review of Microbiology*, 68, 415–438.

Yoon, S., Liu, Z., Eyobo, Y., & Orth, K. (2003). *Yersinia* effector YopJ inhibits yeast MAPK signaling pathways by an evolutionarily conserved mechanism. *The Journal of biological chemistry*, 278, 2131–2135.

Yu, G., Xian, L., Xue, H., Yu, W., Rufian, J. S., Sang, Y., ... Macho, A. P. (2020). A bacterial effector protein prevents mapk-mediated phosphorylation of sgt1 to suppress plant immunity. *PLoS Pathogens*, 16, 1–30.

Zhao, C., Wang, H., Lu, Y., Hu, J., Qu, L., Li, Z., ... Valls, M. (2019). Deep Sequencing Reveals Early Reprogramming of *Arabidopsis* Root Transcriptomes Upon *Ralstonia solanacearum* Infection. *The American Phytopathological Society*, 32, 813–827.

Zurbriggen, M. D., Carrillo, N., & Hajirezaei, M. R. (2010). ROS signaling in the hypersensitive response: When, where and

what for? *Plant Signaling and Behavior*, 5, 393–396.

초록

식물은 내재된 면역체계를 가지고 병원균을 감지하거나 대응한다. Pattern recognition receptor 에 의한 pathogen-associated molecular pattern 의 인식은 PAMP-triggered immunity(PTI)를 유발한다. 해당 면역반응은 빠르고 강력한 활성산소종의 생성과 다양한 유전자의 발현변화를 포함한다. 병원균은 식물의 이러한 면역반응을 피하기 위해 여러 가지 병원성 인자들을 생산한다. 대표적으로 type III secretion system 을 이용하여 세포 내로 직접 주입되는 이펙터 단백질(type-III effector, T3E)이 있다. 이 단백질은 식물에서 effector-triggered susceptibility 를 야기한다. 하지만 식물이 가진 저항성 단백질은 특정 이펙터를 인식하여 effector-triggered immunity 반응을 가져온다. 이 강한 면역반응은 세포 사멸의 형태로 나타나는 과민성 반응을 일으킨다. *Ralstonia solanacearum*(*Rso*)은 가지과 식물에 심각한 풋마름병을 일으키는 병원균이다. *Rso* 는 *Ralstonia*-injected protein(Rip)이라는 다양한 이펙터들을 식물 내로 주입하며 감염을 촉진한다. 본 연구에서는 선행연구에서 클로닝한 50 개의 이펙터 중 세포사멸을 일으키지 않는 36 개의 이펙터를 선별하여 식물에 PTI signaling 에 미치는 영향을 연구하기 위하여 담배(*Nicotiana benthamiana*)에 일시적으로 발현(transient expression)시켰다. 이 이펙터들 중 일부는 flg22 단백질이 유도하는 활성산소종의 생성을 저해하는 것으로 나타났다. 흥미롭게도 이펙터 중 하나인 RipB 의 4 개의 allele 들 중 3 개는 활성산소종의 생성을 거의 완전히 억제하였다. 유전자 서열분석과 키메라를 이용하여

RipB 의 활성산소종 생성 억제제가 이 3 가지의 RipB allele 들의 C-terminal domain 과 관련이 있음을 확인하였다. RipB 는 다른 식물 세균인 *Xantomonas* 와 *Pseudomonas* 의 이펙터인 XopQ 와 HopQ1 의 homolog 단백질이다. 이 두 이펙터를 인식하는 저항성 단백질인 Roq1 의 발현이 억제된 식물에서는 RipB allele 들의 C-terminal 부분이 인식이 되지 않았지만, 여전히 활성산소종의 생성이 억제되었다. 이러한 결과들을 종합해 볼 때, RipB 는 식물의 면역반응을 조절할 수 있는 것으로 보이며 그들이 어떤 경로를 통해 기능하는지를 밝히기 위한 추가적인 연구가 필요할 것이다.

주요어: 활성산소종, *Ralstonia solanacearum*, 담배 (*Nicotiana benthamiana*), 이펙터, PTI, ETI, RipB, 식물 면역

학번: 2019-23541